










## RESEARCH ARTICLE

# Translatome analysis reveals microglia and astrocytes to be distinct regulators of inflammation in the hyperacute and acute phases after stroke

Victoria G. Hernandez<sup>1</sup>  | Kendra J. Lechtenberg<sup>1</sup>  | Todd C. Peterson<sup>1</sup>  |  
Li Zhu<sup>1</sup> | Tawaun A. Lucas<sup>1</sup>  | Karen P. Bradshaw<sup>1</sup>  | Justice O. Owah<sup>1</sup>  |  
Alanna I. Dorsey<sup>1</sup>  | Andrew J. Gentles<sup>2,3</sup>  | Marion S. Buckwalter<sup>1,4</sup> 

<sup>1</sup>Department of Neurology and Neurological Sciences, Stanford School of Medicine, Palo Alto, California, USA

<sup>2</sup>Department of Pathology, Stanford University, Stanford, California, USA

<sup>3</sup>Department of Medicine - Biomedical Informatics Research, Stanford University, Stanford, California, USA

<sup>4</sup>Department of Neurosurgery, Stanford School of Medicine, Palo Alto, California, USA

**Correspondence**

Marion S. Buckwalter, Department of Neurology and Neurological Sciences, Stanford School of Medicine, Palo Alto, CA 94035, USA.  
Email: [marion.buckwalter@stanford.edu](mailto:marion.buckwalter@stanford.edu)

**Funding information**

American Heart Association, Grant/Award Number: 19PABHI34580007; Fondation Leducq, Grant/Award Number: 19CVD01; National Institutes of Health, Grant/Award Numbers: NS067132, T32MH020016; Paul G. Allen Frontiers Group

**Abstract**

Neuroinflammation is a hallmark of ischemic stroke, which is a leading cause of death and long-term disability. Understanding the exact cellular signaling pathways that initiate and propagate neuroinflammation after stroke will be critical for developing immunomodulatory stroke therapies. In particular, the precise mechanisms of inflammatory signaling in the clinically relevant hyperacute period, hours after stroke, have not been elucidated. We used the RiboTag technique to obtain microglia and astrocyte-derived mRNA transcripts in a hyperacute (4 h) and acute (3 days) period after stroke, as these two cell types are key modulators of acute neuroinflammation. Microglia initiated a rapid response to stroke at 4 h by adopting an inflammatory profile associated with the recruitment of immune cells. The hyperacute astrocyte profile was marked by stress response genes and transcription factors, such as *Fos* and *Jun*, involved in pro-inflammatory pathways such as TNF- $\alpha$ . By 3 days, microglia shift to a proliferative state and astrocytes strengthen their inflammatory response. The astrocyte pro-inflammatory response at 3 days is partially driven by the upregulation of the transcription factors *C/EBP $\beta$* , *Spi1*, and *Rel*, which comprise 25% of upregulated transcription factor-target interactions. Surprisingly, few sex differences across all groups were observed. Expression and log<sub>2</sub> fold data for all sequenced genes are available on a user-friendly website for researchers to examine gene changes and generate hypotheses for stroke targets. Taken together, our data comprehensively describe the microglia and astrocyte-specific translatome response in the hyperacute and acute period after stroke and identify pathways critical for initiating neuroinflammation.

**KEYWORDS**

glia, ShinyApp, transcription factor, RNASeq, inflammation

**1 | INTRODUCTION**

Stroke is a leading cause of death and long-term disability worldwide (Virani et al., 2021). Despite its prevalence, existing treatments for

ischemic stroke are limited to restoration of blood flow to the affected brain tissue by using tissue plasminogen activator (tPA) or mechanical methods to remove blockages. This serves to mitigate the extent of initial cell death; however, these interventions are only effective within a narrow time window (<24 h), and other pharmacologic therapies are extremely limited. Neuroinflammation after stroke is a promising therapeutic target because it leads to increased pathophysiology, neurodegeneration and poorer outcomes in the days to months following the initial insult. Unfortunately, clinical trials targeting the overall curtailment of inflammation have been unsuccessful in improving stroke outcomes (Iadecola et al., 2020; Moretti et al., 2015; Stuckey et al., 2021).

To effectively modulate inflammation after stroke to improve outcomes, it is critical to define immune changes in the hyperacute phase that affect the ensuing cascade of molecular processes including inflammation and its resolution and its repair and regeneration. Resolution of inflammation depends on rapid clearance of early damage signals, upregulation of anti-inflammatory cytokines, and removal of dead cells (Shichita et al., 2017), yet the molecular signature of the hyperacute inflammatory response that initiates neuroinflammation after stroke is not known. We do know that this response is largely initiated by brain resident glial cells. Many of the hallmarks of neuroinflammation following stroke—release of pro-inflammatory cytokines, recruitment of immune cells, formation of the glial scar, and modulation of the blood brain barrier (BBB)—are largely initiated by microglia and astrocytes during this hyperacute period. Inhibition or depletion of microglia before stroke results in larger strokes and worse functional outcomes (Lalancette-Hébert et al., 2007; Szalay et al., 2016). However, prolonged or exaggerated microglial activation after stroke is also believed to be detrimental (Iadecola & Anrather, 2011). Astrocytes play a similarly complex role after stroke, both amplifying inflammation (Rakers et al., 2019) and forming a glial scar that can be protective and promote axonal regeneration (Anderson et al., 2016, 2018; Faulkner et al., 2004). The potentially contradictory roles of microglia and astrocytes in neuroprotection after ischemic injury underscore the complex nature of inflammation and how it might divergently impact recovery at different stages following stroke.

For these reasons, we sought to accurately characterize the microglial and astrocytic transcriptome in the hyperacute and acute period after stroke. We achieved this by using a ribosomal pulldown technique to isolate microglia or astrocyte-enriched RNA (Sanz et al., 2009). This strategy eliminates the need to isolate cells by sorting, which can introduce early responses that are similar enough to early injury responses to confound effects (Haimon et al., 2018). The ribosomal pulldown technique also allows for rapid isolation of RNA at a precise time point. We used immunoprecipitation in Microglia RiboTag and Astrocyte RiboTag mice to rapidly isolate actively translating mRNA from cortical tissue. We selected 4 h as a hyperacute time point after stroke as it is a clinically accessible yet very early window in terms of defining the initiation of inflammation, and 3 days as an acute time point when inflammation is well underway, and may serve as a second treatment window for patients unable to receive hyperacute interventions. The distal middle cerebral artery occlusion

model (dMCAO) of ischemic stroke was chosen for this study to model ischemia without reperfusion. The dMCAO model is advantageous due to its accessibility and reproducibility: it results in predominantly cortical strokes and has low variability in stroke size and location (Doyle et al., 2012; Tamura et al., 1981). We analyzed changes in microglial and astrocyte gene expression at a hyperacute and acute time point after stroke and applied differential expression and pathway analysis to identify key features of the microglial and astrocyte response at each of these post-stroke time points. Finally, we constructed a user-friendly web resource for the community to investigate their genes of interest after stroke.

## 2 | METHODS

### 2.1 | Animals

All animal use was in accordance with protocols approved by the Stanford University Institutional Animal Care and Use Committee. *Cx3cr1<sup>CreER</sup>* mice (B6.129P2 (Cg)-*Cx3cr1<sup>tm2.1 (cre/ERT2)</sup>Litt/Wgn*, JAX:021160), *Aldh11<sup>CreER</sup>* (B6N.FVB-Tg (*Aldh11-cre/ERT2*)1Khakh/J, JAX:029655) and *Rpl22<sup>HA</sup>* (B6.129 (Cg)-*Rpl22<sup>tm1.1Psam</sup>/SjJ*, JAX:029977) were purchased from The Jackson Laboratories (Bar Harbor, ME). Mice were housed in a temperature-controlled 12-h light-dark alternating facility, with *ad libitum* access to food and water. All experiments were performed with 10–12-week-old male and female mice. To generate mice with conditional expression of a hemagglutinin (HA) tag on the *Rpl22* ribosomal subunit in microglia and astrocytes, we bred *Cx3cr1<sup>CreER</sup>* and *Aldh11<sup>CreER</sup>* animals with *Rpl22<sup>HA+/+</sup>* animals, respectively. Experimental animals, *Cx3cr1<sup>CreER2-IRES-eYFP/+</sup>;Rpl22<sup>HA+/+</sup>* (Microglia RiboTag) and *Aldh11<sup>CreER2/+</sup>;Rpl22<sup>HA+/+</sup>* (Astrocyte RiboTag) were homozygous for the *Rpl22<sup>HA</sup>* allele and heterozygous for the *CreER* knock-in allele. *Cx3cr1<sup>CreER2-IRES-eYFP/+</sup>;Rpl22<sup>HA+/+</sup>* animals were treated with 200 mg/kg tamoxifen in corn oil via oral gavage on three consecutive days to induce recombination and expression of the hemagglutinin tag. Stroke surgeries were performed 30 days after the last tamoxifen dose. *Aldh11<sup>CreER2/+</sup>;Rpl22<sup>HA+/+</sup>* animals were treated with 80 mg/kg tamoxifen (Srinivasan et al., 2016) in corn oil via oral gavage on five consecutive days to induce recombination and expression of the hemagglutinin tag. Stroke surgeries were performed 8 days after the last tamoxifen dose to ensure tamoxifen and its metabolites were completely degraded (Valny et al., 2016).

### 2.2 | Distal middle cerebral artery occlusion stroke model

Stroke was induced using distal middle cerebral artery occlusion (dMCAO) which has been previously described in detail (Doyle et al., 2012; Tamura et al., 1981). Briefly, animals were anesthetized with 2% Isoflurane in 2 L/min 100% oxygen and an incision was made along the animal's skull, first through the skin and then through the

temporalis muscle. The middle cerebral artery was identified, a craniotomy was drilled, dura was removed, and the artery was cauterized. Sham mice were subject to the same surgical procedure as stroke mice, except that the artery was not cauterized. Mice were randomly placed in stroke or sham groups by alternating the surgery type for each timepoint group. Animals were maintained at 37°C both during surgery and recovery using a feedback-controlled heating blanket. Following surgery, incisions were sealed using Surgi-lock tissue adhesive (Meridian, Allegan, MI). Mice were concurrently injected with 25 mg/kg cefazolin (VWR #89149-888) and 0.5 mg/kg of buprenorphine SR (Zoopharm, Windsor, CO) to prevent infection and for pain management, respectively. Animals were monitored until ambulatory and for infection at the surgical site post-operation. Five mice died during dMCAO surgery due to accidental excessive arterial bleeding, all in the astrocyte RiboTag experiment.

### 2.3 | Immunohistochemistry

Mice were deeply anesthetized with either chloral hydrate (*Cx3cr1<sup>CreER2-IRES-eYFP/+</sup>;Rpl22<sup>HA+/+</sup>* animals) or a ketamine/xylazine cocktail (*Aldh111<sup>CreER2/+</sup>;Rpl22<sup>HA+/+</sup>* animals) and perfused with 0.9% heparinized saline. Brains were collected and drop-fixed in 4% PFA in phosphate buffer for 24 h at 4°C, then preserved in 30% sucrose in PBS. A freezing microtome (Microm HM430) was used to collect 40 µm thick coronal brain sections sequentially into 12 tubes. Brain sections were stored in cryoprotectant medium (30% glycerin, 30% ethylene glycol, and 40% 0.5 M sodium phosphate buffer) at -20°C until processing. Standard immunohistochemistry procedures were used to stain free floating sections. Briefly, sections were blocked with 3% donkey serum (Millipore, #S30-100 mL) for 1 h, then incubated for 15 min in each of streptavidin and biotin blocking solutions (Vector Laboratories, SP-2002). Tissue was then incubated at 4°C overnight in primary antibody: anti-IBA1 (rabbit, 1:1000, Wako 019-19741), biotinylated anti-HA (mouse, 1:500, BioLegend 901505), anti-CD68 (rat, 1:1000, BioRad MCA1957S), anti-GFAP (rat, 1:500, Invitrogen 13-0300), anti-PLIN2 (rabbit, 1:500, Proteintech 15294-1-AP), or anti-IGFBP2 (rabbit, 1:500, Abcam ab188200). GFAP, IBA1, HA, PLIN2, and IGFBP2 were labeled with fluorescent secondary antibodies (donkey anti-rat IgG, 1:200; donkey anti-rabbit IgG, 1:200, Thermo-Fisher A-31573; anti-streptavidin IgG, 1:200, Invitrogen Molecular Probes S-32355), mounted onto glass slides, and cover slipped using Vectashield HardSet Mounting Medium (Vector Laboratories, H-1400). For CD68 staining, tissue was incubated for 1 h in secondary antibody (rabbit anti-rat IgG, 1:500, Vector Laboratories BA-4001) treated with Avidin-Biotin Complex solution (Vector, #PK-6100) for 1 h, and treated for 5 min with filtered DAB (Sigma, #D5905) solution. Finally, sections were mounted onto glass slides, air-dried overnight, and then cover slipped with Entellan (Electron Microscopy Sciences 14800).

### 2.4 | Image acquisition and quantification of HA colocalization

Z-stacks were taken at 40× magnification using a Leica confocal microscope. Three z-stacks per brain section were taken in the peri-infarct region dorsal, lateral, and ventral to the stroke lesion, or in equivalent locations in sham brain sections. Five sections were imaged per mouse. Quantification of colocalization between HA, Iba1, Cx3cr1-eYFP, and GFAP was performed using ImageJ software, and counts were averaged across all images for each animal. Then, we calculated the percentage of HA/Iba1/Cx3cr1 triple-positive cells and HA/GFAP double-positive cells by dividing by the total number of HA + cells to quantify specificity of HA expression. We calculated the percentage of Cx3cr1-eYFP/HA and GFAP/HA double-positive cells out of the total number of GFAP+ cells to quantify efficiency of recombination. All imaging and quantification was performed by an experimenter blinded to the experimental group.

### 2.5 | Ribosome immunoprecipitation and RNA extraction

Mice were deeply anesthetized with chloral hydrate (*Cx3cr1<sup>CreER2-IRES-eYFP/+</sup>;Rpl22<sup>HA+/+</sup>* animals) or a ketamine/xylazine cocktail (*Aldh111<sup>CreER2/+</sup>;Rpl22<sup>HA+/+</sup>* animals) and sacrificed at either a hyperacute (4 h after stroke) or acute (3 days after stroke) time point. Peri-infarct cortical tissue and stroke core or equivalent region of sham tissue was rapidly dissected over a cold, sterile metal block on wet ice. Peri-infarct cortex was defined as the area of cortical tissue within a 2.5 mm radius of the stroke core at the time of dissection. Researchers could not be blinded as it was apparent which samples received a stroke or sham surgery. Immunoprecipitation was performed as previously described (Sanz et al., 2009). Briefly, combined peri-infarct and stroke core brain tissue or equivalent region of sham tissue was homogenized at 3% weight per volume using a Dounce homogenizer in buffer (50 mM Tris, pH 7.5, 100 mM KCl, 12 mM MgCl<sub>2</sub>, and 1% NP-40) containing 100 µg/mL cycloheximide (Sigma), 1 mM DTT, 200 U/mL RNasin (Promega), 1 mg/mL heparin, 1X Protease inhibitors (Sigma) and 1 mM DTT. Homogenates were centrifuged for 10 min at 10,000 rpm and 4°C. A portion of the supernatant was immediately stored at -80°C and subsequently served as the “input” for each sample. The remainder of the supernatant was incubated with anti-HA antibody (1:100, BioLegend 901,502) on a gentle rotator for 4 h at 4°C, followed by addition of 200 µL of Dynabeads Protein G (Invitrogen 10004D) and overnight incubation at 4°C with gentle rotating.

Tubes were placed on a magnetic stand to allow removal of the supernatant, and then polysome-bead-antibody complexes were washed 5X at 4°C with high salt buffer (50 mM Tris, pH 7.5, 300 mM KCl, 12 mM MgCl<sub>2</sub>, 1% NP-40, 1 mM DTT, and 100 µg/mL cycloheximide). Buffer RLT with β-mercaptoethanol (Qiagen RNeasy Micro Kit) was added to the samples immediately after the last wash and tubes

were vortexed to release the polysomes from the beads. Tubes were placed back on the magnetic stand, and supernatant containing the polysomes was stored at  $-80^{\circ}\text{C}$  until RNA extraction. These samples were subsequently designated as immunoprecipitated, or “IP”. For both IP and input samples, genomic DNA was removed, and RNA was extracted according to manufacturer's protocols using an RNeasy Micro Kit (Qiagen) for IP and RNeasy Mini Kit (Qiagen) for input samples.

## 2.6 | Library preparation and RNA sequencing

RNA integrity and concentration was measured by BioAnalyzer (Eukaryote RNA Pico, Agilent). Samples with an RNA integrity number (RIN)  $> 6$  were used for RNA-sequencing (average RIN = 8.5). For microglia samples, polyA-enrichment of 8 ng of total RNA from each replicate was used to prepare a cDNA library using the Smart-Seq2 method (Picelli et al., 2014). Libraries were modified for RNA-sequencing using the Nextera XT DNA Sample Preparation Kit (Illumina) with 200 pg of cDNA as starting material. Library quality was assessed by Qubit fluorometer (high sensitivity dsDNA, ThermoFisher), BioAnalyzer (high sensitivity DNA, Agilent), and TapeStation (high sensitivity DNA, Agilent). Sequencing was performed on the Illumina HiSeq 4000 platform to obtain 150 bp paired-end reads. The astrocyte samples were sent to Azenta (formerly GeneWiz) for library preparation, using the NEBNext Ultra RNA Library Preparation Kit with polyA selection. Sequencing was performed on the Illumina HiSeq 4000 platform to obtain 150 bp paired-end reads.

## 2.7 | RNASeq data processing and analysis

Approximately 12–36 million 150 bp reads were obtained from all microglia and astrocyte samples. These reads were trimmed of adapter sequences, low quality bases, and very short reads using trimGalore! (v0.4.5), a wrapper script which utilizes cutadapt (Martin, 2011) and FastQC (v0.11.7). Remaining reads were aligned to the mouse mm10 genome (GRCm38.p6) using the STAR aligner (Dobin et al., 2013) (v2.7.1), which utilizes an algorithm that minimizes alignment time, mapping errors, and alignment biases. Transcript abundances were then annotated and quantified using the RSEM software package (B. Li & Dewey, 2011) (v1.3.1). Differential gene expression analysis was carried out using the DESeq2 (Love et al., 2014) (v1.26) package within the R environment. The “apeglm” method was used to shrink log fold change calculations (Zhu et al., 2019). A significance cutoff was set using the adjusted  $p$  value  $< .05$  and  $|\log_2\text{fold change}| > 1$ . Transcripts with low abundances ( $< 10$  counts for any of the samples) were excluded from analysis. Predicted pseudogene (Gm-) and RIKEN cDNA gene (–Rik) transcripts were removed for downstream analysis. Plots were generated using ggplot2 (v3.2.1). Gene ontology analysis was performed using DAVID (version 6.8) to identify biological processes and KEGG pathways enriched after stroke (Huang et al., 2009a; 2009b).

## 2.8 | Group sizes and inclusion/exclusion criteria

The study was powered to detect differences between sexes as well as sham/stroke, based upon discussions with biostatisticians in the Stanford Genomics Bioinformatics Service Center and based upon a pilot RNAseq experiment performed using microglia-enriched RNA from Cx3cr1-CreER-IRES-eYFP/+;Rpl22-HA+/+ sequenced on the Illumina MiSeq platform. We eliminated some samples based on principal component analysis of the top 500 expressed genes. Four microglia samples presented as extreme outliers, and experimental notes indicated that these particular brain samples appeared abnormal at the time of dissection (e.g. a. large hemorrhage in a sham brain, no visible stroke in a “stroke” brain). These were excluded. In the astrocyte experiment, four sequenced 4 h sham IP samples clustered with the 4 h stroke IP samples in our initial run with a group size of six. To address this, we repeated all groups. In the new cohort, 4 h sham samples clustered with the other 4 h sham samples and the other groups clustered as expected. All were included in the analysis except the four mis-clustered sham samples from cohort 1. Thus, the total number of microglia RiboTag mice included were as follows: 4 h sham, five male, four female; 4 h stroke, five male, six female; 3 day sham, five male, five female; 3 day stroke, six male, six female. For astrocyte RiboTag, final group sizes were as follows: 4 h sham, eight male, four female; 4 h stroke, 10 male, 10 female; 3 day sham, eight male, eight female; 3 day stroke, eight male, eight female.

## 2.9 | Gene set enrichment analysis and gene list generation

Published lists of upregulated genes from various recent microglia and astrocyte gene expression studies were downloaded and used for analysis (Table 1). To generate gene sets, the published gene sets were filtered to only include genes upregulated with a fold-change  $> 1.5$  and adjusted  $p$  value, or false discovery rate (FDR)  $< 0.05$ . Gene Set Enrichment Analysis (GSEA) was run on full stroke IP gene lists which were ranked based on transcripts per million (TPM) using GSEA software (version 4.0.1) (Mootha et al., 2003; Subramanian et al., 2005), and GSEA was performed using 1000 permutations, weighted enrichment statistic, and Signal2Noise ranking metric against manually uploaded gene lists (Table 1).

## 2.10 | Cell isolation for flow cytometry

Mice were deeply anesthetized 3 days after dMCAO stroke surgery, approximately 0.6 mL whole blood was obtained by cardiac puncture, and then animals were transcardially perfused with cold heparinized 0.9% saline. Brains were then extracted and split into hemispheres, and cerebellum and olfactory bulbs were removed. White blood cells were obtained by red blood cell lysis and resuspension of approximately  $10^6$  cells in 200 mL of HBSS. The brain hemisphere ipsilateral to the stroke was homogenized in 10 mL HBSS, filtered through a 70  $\mu\text{m}$  cell strainer, and then digested in collagenase IV (1 mg/mL,

**TABLE 1** Sources and criteria for microglia and astrocyte gene sets for Gene Set Enrichment Analysis (GSEA).

Dataset name	Reference	Filtering criteria used
Disease-associated microglia cluster	Keren-Shaul et al. (2017) Table S3, mmc3	FC >1.5; $p < .05$
Aged microglia cluster	Hammond et al. (2019), Table S1, Cluster OA2	FC >1.5; FDR < 5E-88
Demyelination-injury-responsive microglia cluster	Hammond et al. (2019), Table S1, Cluster IR2	FC >1.5; FDR < 4E-106
LPS-responsive versus adult microglia	Bennett et al. (2016), Dataset S01, Adult to LPS	FC >1.5; FDR <0.05
2 days post-TBI vs. sham microglia	Izzy et al. (2019), Table S1	FC >1.5; $q < 0.05$
14 days post-TBI versus sham microglia	Izzy et al. (2019), Table S2	FC >1.5; $q < 0.05$
60 days post-TBI versus sham microglia	Izzy et al. (2019), Table S3	FC >1.5; $q < 0.05$
End-stage versus aged control microglia	Chiu et al. (2013), Table S3	FC >1.5; FDR <0.05
LPS versus PBS microglia	Sousa et al. (2017), Data EV1	FC >1.5; FDR <0.05
3 h LPS-specific vs saline astrocytes	Hasel et al. (2021), Table S2	FC >2; FDR <0.05
24 h LPS-specific vs saline astrocytes	Hasel et al. (2021), Table S2	FC >2; FDR <0.05
72 h LPS-specific versus saline astrocytes	Hasel et al. (2021), Table S2	FC >2; FDR <0.05
2 year old versus 10 week cortical astrocytes	Clarke et al. (2018), Dataset S3	FC >2; FDR <0.05; FPKM $\geq 5$ in 2-year-old samples for upregulated genes
EAE versus unimmunized astrocytes	Borggrewe et al. (2021), Table S5	FC >2; FDR <0.05
Alzheimer's disease vs wild type astrocytes	Orre et al. (2014), Table 1	Top 50 upregulated genes, FDR <0.05
3 day tMCAO versus sham astrocytes	Rakers et al. (2019), Table S1	FC >1.5; FDR <0.05
24 h tMCAO versus sham astrocytes	Zamanian et al. (2012), Table 1	Top 50 upregulated genes, FDR <0.05
SOD1 versus wild type	Sun et al. (2015), Table S4	FC >0.5; FDR <0.05
2 year versus 4 month old visual and motor cortex astrocytes	Boisvert et al., (2018), Table S3	FC >1.5; FDR <0.05

Worthington, Lakewood, NJ) with DNase in HBSS for 30 min at 37°C with 200 rpm shaking. Myelin was removed by addition of 5 mL of 30% Percoll (Sigma) in PBS and density-gradient centrifugation, and cells were washed in serum-supplemented DMEM. Dead cells were labeled using Live/Dead fixable aqua dead cell staining kit (ThermoFisher Scientific). Cells were fixed for 20 min in cold Fixation/Permeabilization buffer (BD Biosciences) then washed, and stored in fetal bovine serum containing 10% DMSO at -80°C.

### 2.11 | Flow cytometry analysis

Approximately  $10^6$  brain cells and  $0.5 \times 10^6$  blood cells were used for flow cytometry analysis. Fc receptors were blocked with 100 mL solution containing anti-mouse CD16/CD32 (1:100, BD Pharmingen, 553,141) for 30 min at 4°C. Cells were washed and permeabilized for intracellular staining in Perm/Wash Buffer (BD Biosciences) and antibody staining was performed in 100  $\mu$ L Perm/Wash buffer for 30 min at 4°C. The following antibodies were used for surface receptor labeling: CD45 (1:200, BioLegend, 103112), CD11b (1:200, BioLegend, 101216), HA (1:200, BioLegend, 901517), Ly6G (1:200, BioLegend, 127623), and Cx3cr1 (1:200, BioLegend, 149009). Cells were washed in buffer and analyzed with an LSR II cytometer (BD Biosciences). Gating and analysis of cell populations was carried out using FlowJo software (Tree Star Inc.).

### 2.12 | Statistical analysis

Quantified immunohistochemistry data was analyzed using a two-way ANOVA with Tukey's multiple comparisons test for post-hoc analysis in GraphPad Prism 8 software. All data are presented as mean  $\pm$  SEM unless indicated. Experiments were designed using power analyses to determine sample sizes based on expected variances and group differences. All animals were randomized between experimental groups and experimenters were blinded to group assignments during analysis. Spearman correlation was calculated from the mean TPM values of genes. Z-scores were calculated across all IP samples for other heatmap representations. TPM values were not used for statistical analysis.

## 3 | RESULTS

### 3.1 | Characterization and validation of microglia and astrocyte RiboTag mice for cell-specific isolation of RNA after stroke

To isolate the microglia or astrocyte-specific gene expression signature after stroke, we took advantage of the genetic RiboTag technique. This allows for immunoprecipitation of ribosomes from a cell type of interest, so that the actively translating mRNA transcriptome

can be isolated based on cell-type specific promoters. The *Cx3cr1* promoter used in our Microglia RiboTag mice (*Cx3cr1<sup>CreER2-IRES-eYFP/+</sup>; Rpl22<sup>HA+/+</sup>*) (Figure 1A) is also expressed by some peripheral immune cells, including monocytes and some T cells (Böttcher et al., 2015; Mionnet et al., 2010; Steffen et al., 2000). To ensure microglial-enriched mRNA and exclude infiltrating myeloid cells at the time of stroke, we allowed for 30 days to elapse between the last tamoxifen dose and stroke or sham surgery in Microglia RiboTag mice (Figure 1B). Given that peripheral immune cell populations turn over relatively quickly (Gu et al., 2016; Parkhurst et al., 2013), a 30 day wait period ensures that no peripheral *Rpl22<sup>HA</sup>*-expressing cells remain after tamoxifen administration in Microglia RiboTag mice (Figure S1). Microglia RiboTag mice are haploinsufficient for the fractalkine receptor, but we did not observe significant weight loss after stroke (data not shown). Additionally, loss of this receptor did not affect stroke size or microglia/macrophage activation, measured by quantification of immunostaining for the microglia/macrophage activation marker CD68 (Figure S2). The *Aldh111* promoter is highly specific to astrocytes (Hu et al., 2019), thus we only implemented an 8 day waiting period between the last tamoxifen dose and stroke or sham surgery in our Astrocyte RiboTag mice (*Aldh111<sup>CreER2/+</sup>; Rpl22<sup>HA+/+</sup>*) (Srinivasan et al., 2016), to ensure tamoxifen and its metabolites were completely degraded (Valny et al., 2016).

To verify faithful HA expression in our cell types of interest, we used fluorescence confocal microscopy to colocalize HA and cell-

specific markers in brain sections from Microglia RiboTag or Astrocyte RiboTag mice 3 days after stroke. Almost all HA immunostaining (99%) colocalized with microglia markers *Iba1* and *Cx3cr1*, indicating high specificity of the *Rpl22* tag (Figure 1c,d). In Astrocyte RiboTag mice, 100% of HA-expressing cells co-localized with the astrocyte marker GFAP, and 98% of GFAP-expressing cells also express HA, validating that the HA tag is efficiently expressed specifically in astrocytes in this mouse line (Figure 1e,f).

### 3.2 | Isolation and sequencing of microglia and astrocyte-enriched mRNA at hyperacute and acute timepoints after ischemic stroke

To isolate mRNA reflecting the immune response to stroke, we immunoprecipitated microglia-enriched (microglia-IP samples) and astrocyte-enriched (astrocyte-IP samples) mRNA from the stroke core and 2–3 mm of surrounding peri-infarct cortex at 4 h and 3 days after dMCAO stroke or sham surgery. In addition, we isolated RNA from the non-immunoprecipitated homogenate (Input samples) to assess overall gene expression and further validate the cell-specificity of our RiboTag mouse lines. For each of the two time points, we sequenced microglia-IP mRNA samples from 9 to 12 individual adult mice after stroke or sham surgery (Figure 2a). For the astrocyte-IP cohort, we sequenced samples from 12 to 20 individual adult mice after dMCAO

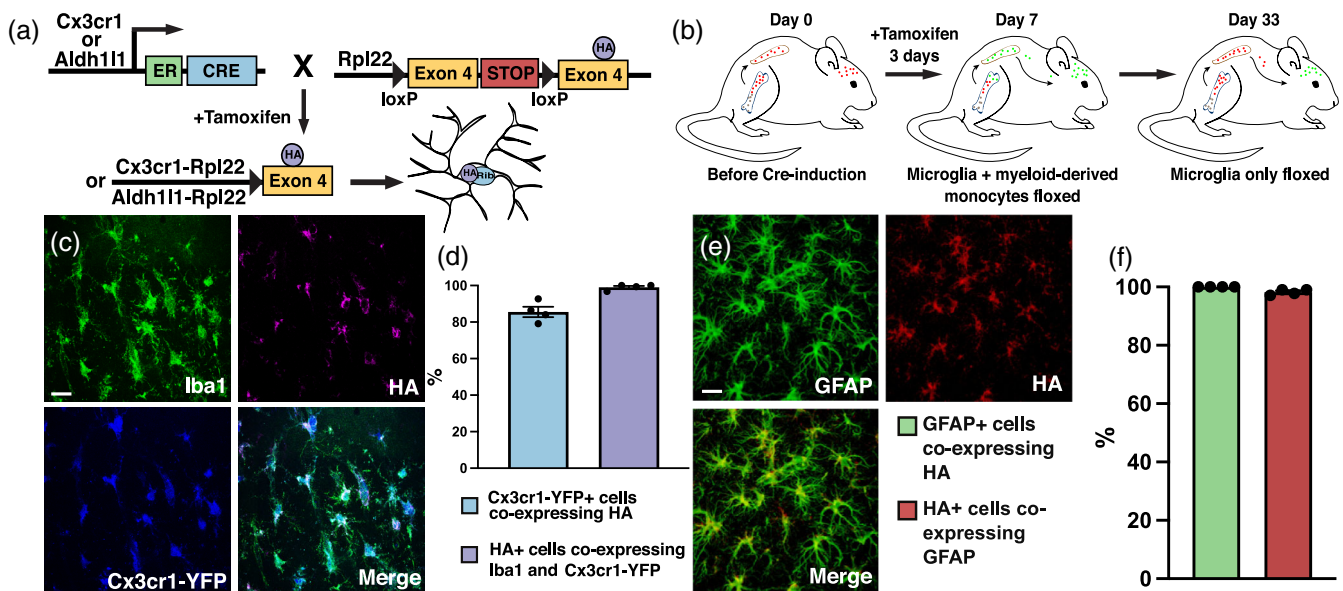


**FIGURE 1** Characterization of microglia and astrocyte-RiboTag mice for isolation of microglial or astrocytic RNA after stroke. (a) Strategy for breeding and inducing Microglia-RiboTag (*Cx3cr1<sup>CreER2-IRES-eYFP/+</sup>; Rpl22<sup>HA+/+</sup>*) and Astrocyte-RiboTag (*Aldh111<sup>CreER2/+</sup>; Rpl22<sup>HA+/+</sup>*) mice. (b) Strategy for isolating microglia from peripheral cells in Microglia-RiboTag mice. (c) Representative immunofluorescence images for HA and microglia-specific markers taken in cortex of Microglia-RiboTag mice 3 days after dMCAO stroke. (d) Quantification of the specificity of HA by microglia and efficiency of recombination in Microglia-RiboTag mice. (99.0% ± 0.8%,  $n = 3-4$ ). Recombination occurred in the majority of *Cx3cr1*+ cells quantified, and after stroke, 85.6% ± 2.8% *Cx3cr1*+ cells were HA+ ( $n = 4$ ). 150 *Iba1*+ cells per mouse. Scale bar = 20  $\mu$ m. (e) Representative immunofluorescence images for HA and astrocyte-specific marker taken in cortex of Astrocyte-RiboTag mice 3 days after dMCAO stroke. (f) Quantification of the specificity of HA by astrocytes and efficiency of recombination in Astrocyte-RiboTag mice. Almost all HA+ cells co-expressed GFAP in stroke condition (100% ± 0%,  $n = 4$ ). Recombination occurred in the majority of GFAP+ cells quantified, after stroke, 98.2% ± 0.47% GFAP+ cells were HA+ ( $n = 4$ ). 100 GFAP+ cells per mouse. Scale bar, 20  $\mu$ m; error bars, SEM.

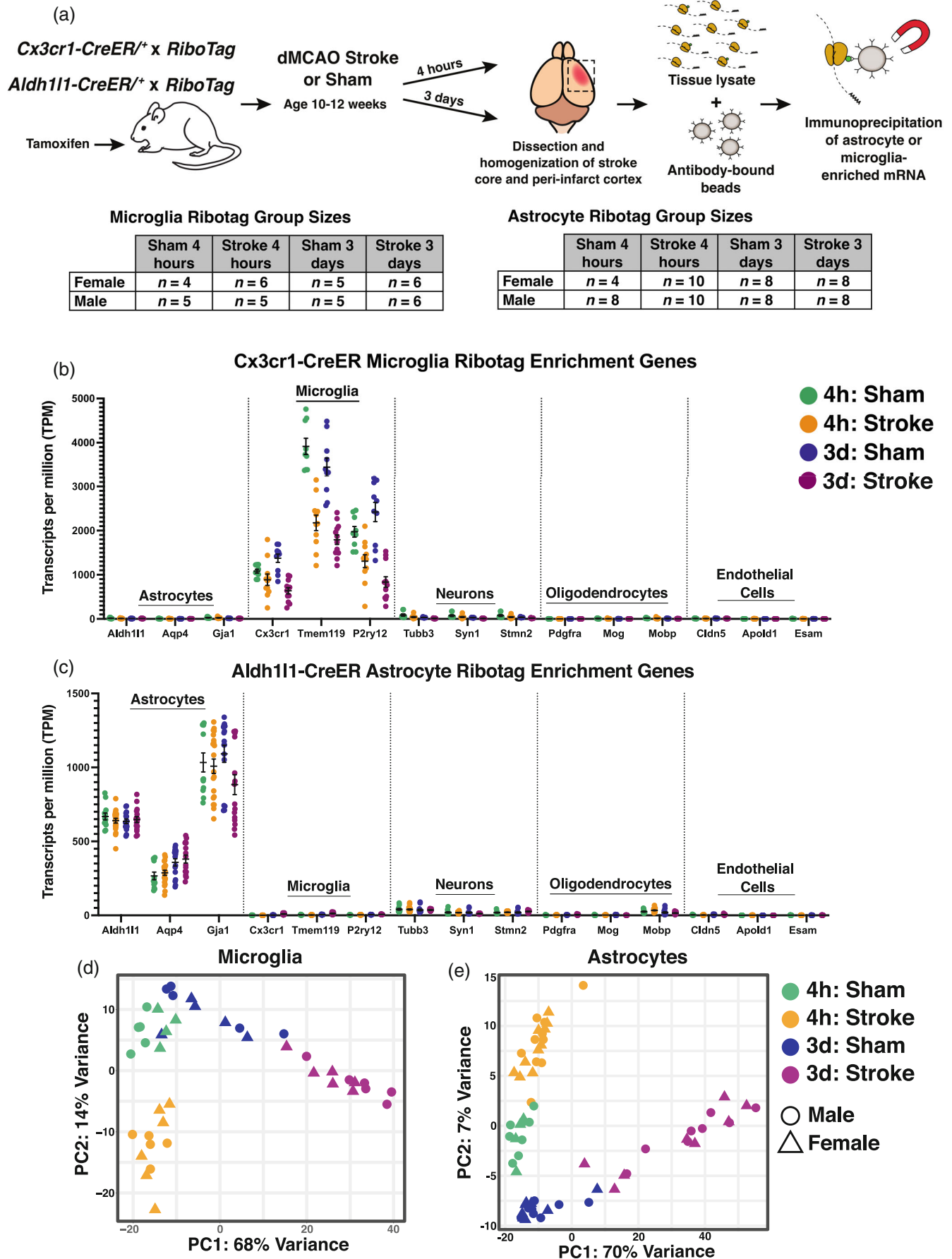


FIGURE 2 Legend on next page.

stroke or sham surgery (Figure 2a). Half the animals used for this study were male and half were female to allow us to examine sex-specific changes in microglial and astrocyte gene expression after ischemic stroke.

To validate cell-specificity in the RNAseq data we examined cell-specific genes encompassing astrocytes, microglia, neurons, oligodendrocytes, and endothelial cells. We analyzed the expression levels of canonical brain cell markers in microglia-IP samples and astrocyte-IP samples in all four experimental groups: 4 h and 3 day, and sham and stroke. We observed high cell-specificity in IP samples from both mouse lines (Figure 2b,c). Principal component analysis also demonstrated distinct separation of the 4-h sham, 4-h stroke, 3-day sham, and 3-day stroke groups in both cell types. The first two principal components accounted for 82% of the variance in gene expression among the microglia-IP samples (Figure 2D) and 77% for the astrocyte-IP samples (Figure 2E). Interestingly, for both microglia and astrocytes, the 3-day stroke and sham groups separated along a continuum in the first principal component, whereas the 4-h stroke and sham samples clustered into discrete groups in the second principal component.

### 3.3 | Differential gene expression analysis of microglial and astrocyte transcripts at two time points after stroke

To interrogate how stroke drives transcriptome changes, we identified differentially expressed genes (DEGs) at 4 h and 3 days in microglia and astrocytes using the criteria of adjusted  $p$  value ( $p$ -adj) < .05, and  $|\text{Log}_2$  fold change| > 1 comparing stroke versus sham. In microglia, differential expression analysis between the stroke and sham groups identified 204 unique upregulated genes and 27 downregulated genes at 4 h, and 828 upregulated genes and 608 downregulated genes at 3 days (Figure 3A). In astrocytes, we identified 99 unique upregulated genes and five downregulated genes at 4 h, and 1630 upregulated genes and 94 downregulated genes at 3 days (Figure 3B). Interestingly, the gene changes induced by stroke were fairly distinct at each timepoint in both cell types. In microglia, only 132 upregulated and four downregulated genes were shared between the 4 h and 3 day timepoints. In astrocytes, the two timepoints only shared 234 upregulated genes and no downregulated genes. While the 3 day time point had a greater number of overall differentially expressed genes compared to the 4 h time point, both microglia and astrocytes upregulated more genes than downregulated for each time point (Figure 3c-f).

### 3.4 | Sex differences in the microglia and astrocyte transcriptome after ischemic stroke

Interestingly, in both microglia and astrocytes, male and female samples did not cluster separately in the principal components analysis (Figure 2d,e), so we included all samples regardless of sex in the stroke vs. sham differential expression analysis (Figure 3). However, since stroke induces so many gene changes, it was possible that stroke-induced transcriptional changes might be masking sex differences in the principal components analysis. Therefore, to further investigate the effect of sex on translational changes in microglia-IP and astrocyte-IP samples after stroke, we directly compared female vs. male samples within each of the four experimental conditions. Surprisingly, there were still relatively few gene expression differences between female and male mice in stroke or sham conditions at both time points, and in both microglia and astrocytes (Figure 4a,b). Five sex-chromosome-linked genes, *Xist*, *Kdm5d*, *Uty*, *Ddx3y*, and *Eif2s3y*, were different in all conditions in both cell types while *Ubal5* was different across all conditions in only astrocytes. In the 4 h sham group, only five genes in microglia and astrocytes were differentially expressed between females and males (Figure 4c,d). In the 4 h stroke group, only three genes were differentially expressed in microglia (Figure 4e), while none were differentially expressed in astrocytes. The 3 day sham condition also exhibited few differences, with only three genes in microglia and 1 gene in astrocytes that were differentially expressed between females and males (Figure 4f,g). Sex had the greatest effect on the microglial transcriptome at 3 days after stroke, and interestingly, 77.8% of the genes that were different between females and males were upregulated in females (Figure 4h). These included the genes *Kcnt2*, *Scn8a*, and *Cacnb4*, which are known to be involved in regulation of synaptic transmission and potentiation. Conversely, in astrocytes 3 days after stroke there were few differences with only 1 differentially expressed gene in females versus males (Figure 4i).

### 3.5 | The microglia and astrocyte transcriptomes reflect distinct functions during the hyperacute and acute phases of neuroinflammation after ischemic stroke

To investigate the hyperacute and acute gene expression signature unique to microglia and astrocytes after ischemic stroke, we explored

**FIGURE 2** Isolation and sequencing of microglia and astrocyte-enriched mRNA at multiple time points after ischemic stroke. (a) Schematic depicting the experimental strategy for isolating actively translating microglial or astrocyte RNA at multiple time points after ischemic stroke, and number of biological replicates used for RNA-sequencing. All adult mice (10–12 weeks old at time of surgery) received tamoxifen prior to stroke or sham. Microglia-RiboTag mice received tamoxifen 3 days *p.o.* 30 days before surgery. Astrocyte-RiboTag mice received tamoxifen 5 days *p.o.* 8 days before surgery. Mean TPM values indicating that (b) microglia-IP samples are enriched in microglia-specific genes, (c) Astrocyte-IP samples are enriched in astrocyte-specific genes, and (b,c) de-enriched for cell-specific markers for other brain cell types. Bars,  $\pm$ SEM. (d) Principal component analysis (PCA) of log-transformed RNA-seq data from 4 h and 3 day stroke and sham microglia-IP samples ( $n = 9$ –12 mice per group). (e) Principal component analysis (PCA) of log-transformed RNA-seq data from 4 h and 3 day stroke and sham astrocyte-IP samples ( $n = 12$ –20 mice per group).





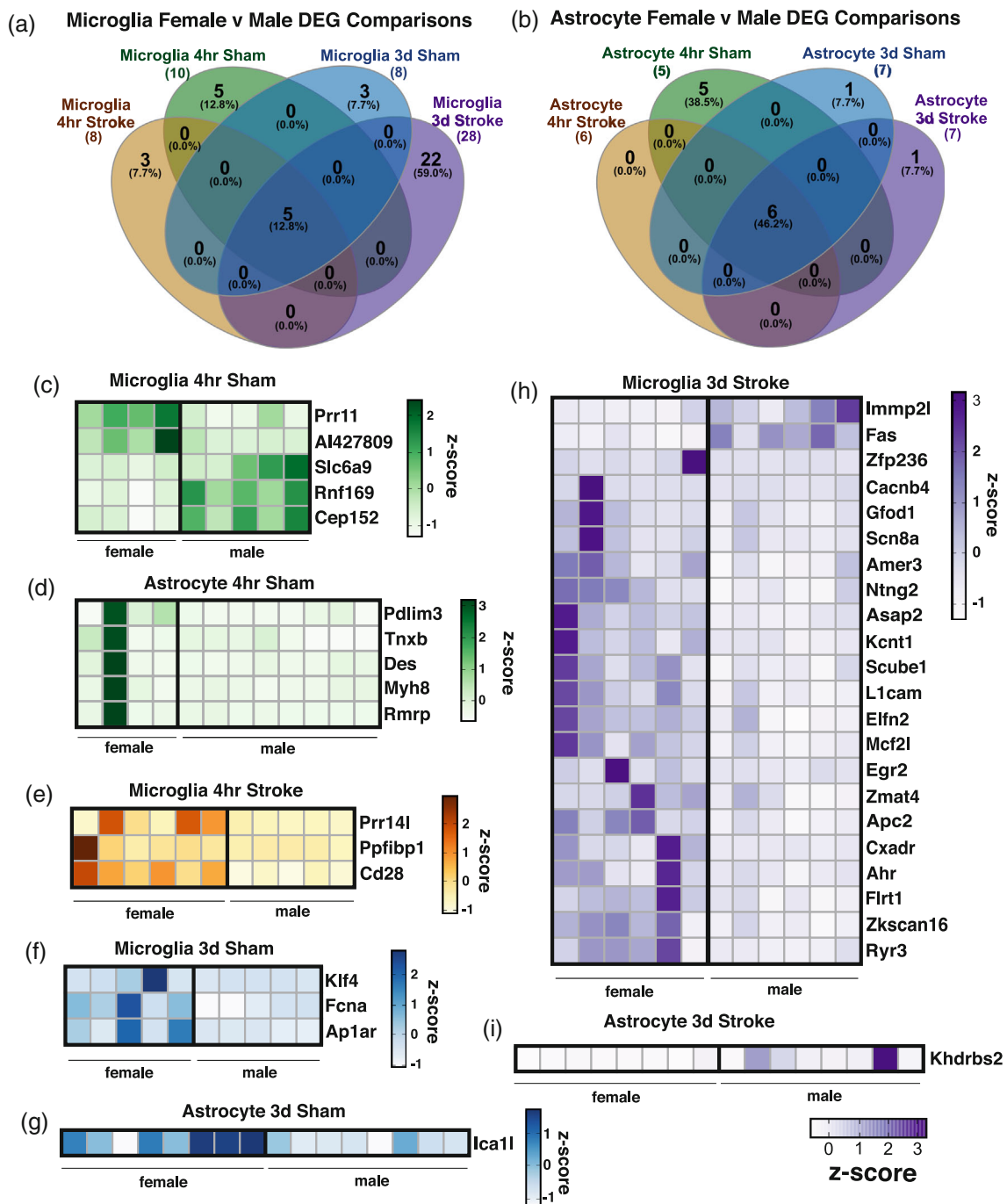


**FIGURE 4** Sex differences in the microglia and astrocyte transcriptomes after ischemic stroke. Number of differentially expressed genes ( $p$  adj  $< .05$ ;  $|\text{Log}_2\text{FC}| > 1$ ) between males and females at 4 h or 3 days after stroke or sham surgery in (a) microglia-IP samples and (b) astrocyte-IP samples. Heatmaps depict expression levels of significantly different genes between female and male mice unique to 4 h after dMCAO sham (c,d) or stroke surgery (e) and 3 days after dMCAO sham (f,g) or stroke surgery (h,i). Sex-linked genes differentially expressed by sex across all conditions were excluded from heatmaps (*Uba1y*, *Ddx3y*, *Kdm5d*, *Eif2s3y*, *Uty*, *Xist*). z-scores were calculated from TPM normalized gene expression values. DEG, differentially expressed genes.

the transcripts which met the criteria of being greater than 2-fold enriched in stroke versus sham conditions at 4 h and 3 days after stroke (and significant,  $p$ -adj  $< .05$ ). With the exception of microglia at 3 days, the number of significant downregulated genes was small ( $< 100$ ) across conditions, thus we decided to primarily focus our

analysis on upregulated genes. The top upregulated genes at the hyperacute and acute timepoints suggest that microglia and astrocytes are engaged in distinct functions during the two time points. During the initiation phase of neuroinflammation after stroke, measured at 4 h after stroke, the most highly up-regulated genes

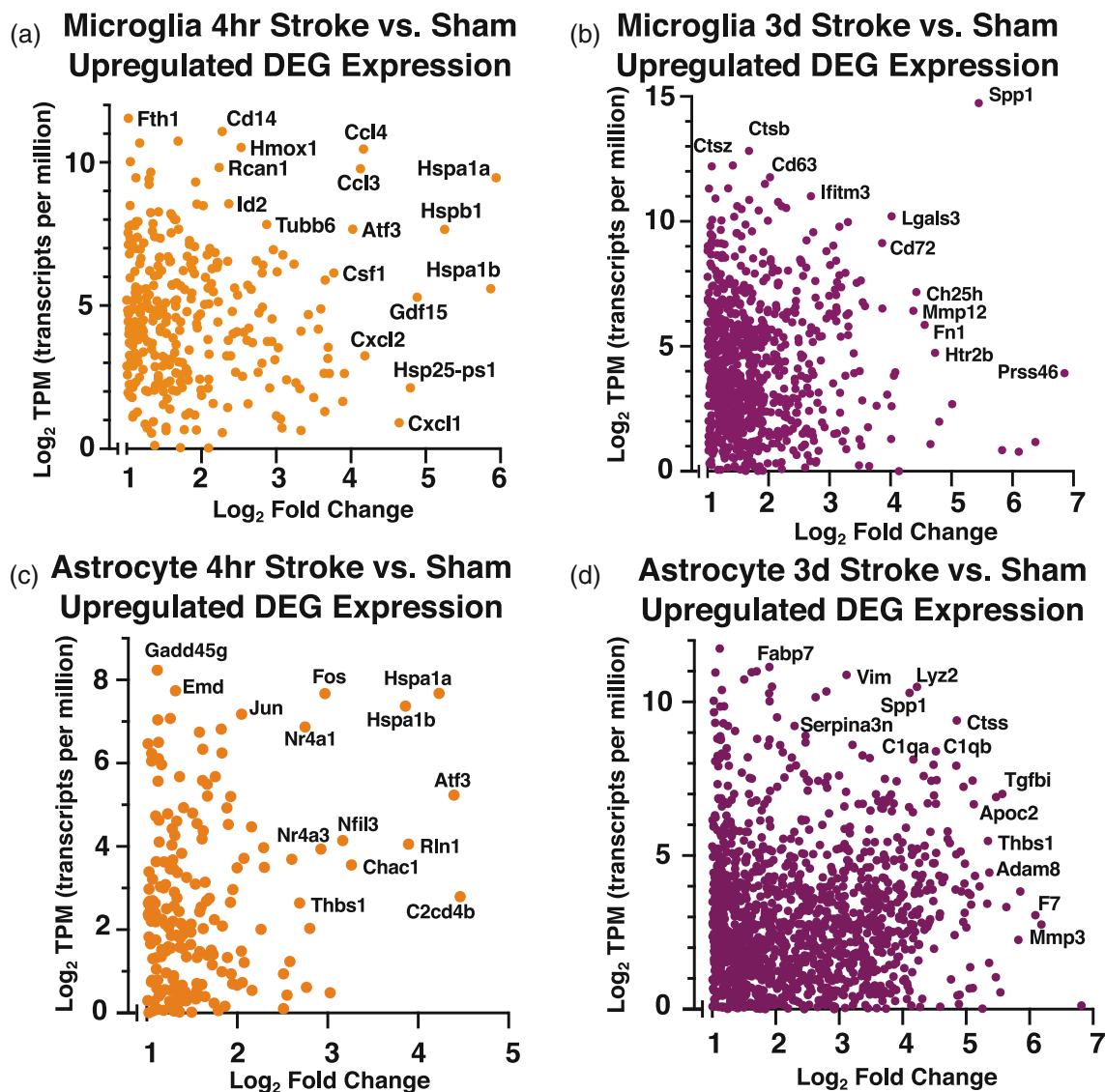


**FIGURE 5** The microglia and astrocyte transcriptomes reflect distinct functions during the hyperacute and acute phases of neuroinflammation after ischemic stroke. Scatter plots for microglia-IP (a,b) and astrocyte-IP (c,d) log<sub>2</sub> mean normalized expression values (TPM) and log<sub>2</sub> fold change for each significantly upregulated differentially expressed gene at 4 h (a,c) and 3 days (b,d) after stroke compared to sham. TPM values used for this representation are the mean TPM for each gene across all samples within respective 4 h and 3 day stroke groups. Highly expressed and/or differentially genes are labeled. Genes with TPM <1 were excluded.

(Figure 5A) in microglia were the heat shock proteins *Hspa1a*, *Hspa1b*, the chemokines *Cxcl1*, *Cxcl2*, and macrophage inflammatory proteins *Gdf15* and *Ccl4*. These gene changes likely reflect a marked microglial response to stress and damage associated molecular patterns (DAMPs) in the ischemic region early after injury. Heat shock protein expression also likely propagates the damage signal and the inflammatory response in the injured tissue. Of the microglia genes which were most significantly regulated by stroke, *Ccl4* and *Ccl3* were expressed at very high levels, suggesting that they may be central features of the microglial stroke response at this time point.

At 3 days after stroke, many more genes were upregulated to a higher expression level than at 4 h after stroke (Figure 5A,b). In microglia during the acute phase at 3 days after stroke, *Spp1* (osteopontin 1)

was highly upregulated and also had a higher expression level than any other gene at the 3 day time point (Figure 5B). *Spp1* is upregulated in degenerative disease-associated microglia (DAM) (Keren-Shaul et al., 2017), is upregulated in the brain after ischemia, and is correlated with phagocytosis (Shin et al., 2011). Other genes which were highly upregulated during the acute phase of neuroinflammation after stroke included *Lgals3* (galectin 3), which promotes microglial proliferation (Rahimian et al., 2018), and *Mmp12* (matrix metalloproteinase 12), which has been associated with worse neuronal damage after stroke (Chelluboina et al., 2015). Upregulation of phagosome-associated genes such as *Ch25h* (cholesterol 25-hydroxylase), *Msr1* (macrophage scavenger receptor 1), and complement C3 indicate that microglia regulate acute inflammation after stroke by phagocytosing

dead cells and debris. *Ch25h* also plays an important role in lipid metabolism, and has been linked to risk for Alzheimer's disease (Papassotiropoulos et al., 2006), suggesting microglia are processing lipids engulfed during debris clearance. *Plin2* (perilipin-2), a gene involved in lipid droplet formation, was also upregulated at this time-point. In addition to regulating adipose tissue, *Plin2* has been thought to drive microglial inflammation after exposure to LPS, aging, EAE, and stroke (Arbaizar-Rovirosa et al., 2023; Khatchadourian et al., 2012; Loix et al., 2022; Marschallinger et al., 2020). There is limited data on the role of microglial *Plin2* after cerebral stroke, thus we validated its expression with fluorescence immunohistochemistry in the peri-infarct cortical region 3 days after stroke (Figure S3A–C).

In astrocytes, the top upregulated genes at the hyperacute and acute time points indicate that astrocytes initiate a stress response as early as 4 h that continues at 3 days. At 4 h, astrocytes highly expressed and highly upregulated (Figure 5C) *Hspa1a* and *Hspa1b*, which encode Hsp70, a chaperone protein that may be neuroprotective after stroke (J. Y. Kim et al., 2020). Another highly expressed stress-response gene, *Gadd45g* (growth arrest and DNA damage inducible gamma), has increased gene and protein expression after tMCAO in mice and may predict poor outcomes after stroke in people (Simats et al., 2020). Astrocytes also upregulated a number of transcription factors at 4 h, including *Fos*, *Jun*, *Atf3*, and *Nfil3*.

Unsurprisingly, at 3 days after stroke, two of the most highly expressed genes in astrocytes are involved in astrogliosis: *Gfap* (glial fibrillary acidic protein) and *Vim* (vimentin) (Figure 5D). Other top expressed and upregulated genes included *Il-6* (interleukin 6) and *Mmp10* (matrix metalloproteinase 10) which are cellular senescence-associated secretory proteins in Alzheimer's disease (Behfar et al., 2022). Another matrix metalloproteinase, *Mmp3*, is also upregulated and has been associated with increased blood brain barrier damage and greater neuroinflammatory response (Yang & Rosenberg, 2015). *Ctsd* and *Ctss* (cathepsins D and S) are also upregulated at 3 days. This could indicate astrocytes have increased extracellular matrix degradation capabilities at 3 days after stroke. In addition, *Igfbp2* (insulin-like growth factor binding protein 2) was highly upregulated and has been implicated in reactive astrogliosis after injury (Hammarberg et al., 1998). Specifically after stroke, *Igfbp2* has been thought to limit neuronal death through binding of *Igf1* (insulin-like growth factor 1) (Beilharz et al., 1998), which was upregulated in our microglial data at 3 days. We validated the protein expression of *Igfbp2* with fluorescence immunohistochemistry in the peri-infarct cortex 3 days after stroke (Figure S3C–F) and found it to be highly specific to astrocytes in the glial scar. Overall, upregulated astrocyte genes at 3 days may be playing a role in blood brain barrier function and glial scar regulation.

### 3.6 | Comparisons to other glial states and disease models

At 3 days post-stroke, we observed a downregulation of microglial signature gene *P2ry12*, leading us to ask if microglia maintain their homeostatic gene expression signature after cerebral ischemia. We

examined expression levels of select microglia signature genes and monocyte/macrophage signature genes compiled from previous studies (Butovsky et al., 2014; Hickman et al., 2013). Many homeostatic microglial signature genes, such as *Tmem119*, *P2ry12*, *Sall1*, and *Gpr34* were downregulated at both 4 h and 3 days after ischemic stroke (Figure 6A). Downregulation of these signature genes was most pronounced 3 days after stroke, and expression levels of additional microglial signature genes, such as *Cx3cr1*, *Hexb*, and *Slc2a5*, were reduced at this time point. Consistent with previous reports, we observed that downregulation of the homeostatic microglial gene expression signature corresponded to upregulation of characteristic macrophage genes (Bohlen et al., 2017; Buttgerit et al., 2016). At 3 days after stroke, microglia strongly upregulated genes associated with macrophage activation/identity including *Fn1*, *Cd51*, and *Saa3* (Figure 6B) (Hickman et al., 2013). Our data indicate that as early as 4 h after stroke, microglia lose their homeostatic gene expression identity and shift towards a macrophage-like phenotype.

We also compared changes in response to stroke in pan-reactive, A1, and A2 astrocyte genes (Liddel et al., 2017). All pan-reactive genes were significantly upregulated in astrocytes at 3 days, with only five being upregulated at 4 h (*Steap4*, *S1pr3*, *Hspb1*, *Cd44*, *Osmr*) (Figure 6C). A1 genes, defined as a subset of neurotoxic genes in response to neuroinflammation, were largely unchanged in astrocytes at 4 h, with the exception of *Gbp2* and *Srgn* being upregulated. Three days after stroke, more than half of A1 genes were upregulated (*H2-T23*, *H2-D1*, *Ggta1*, *Iigp1*, *Gbp2*, *Psm8*, *Srgn*) (Figure 6D). About half of the A2 genes, defined as neurotrophic reactive astrocyte genes, were upregulated at 4 h (*Ptx3*, *Ptgs2*, *Emp1*, *Slc10a6*, *B3gnt5*, *Cd14*), and all but *Sphk1* were upregulated 3 days after stroke (Figure 6E). We did not observe downregulation of any pan-reactive, A1, or A2 genes in either timepoint.

The downregulation of signature microglial homeostatic genes is a hallmark of disease-associated microglia (DAM). The DAM phenotype is observed in mouse models of Alzheimer's disease (AD), tauopathy, ALS, MS, and aging (Jordão et al., 2019; Keren-Shaul et al., 2017; Krasemann et al., 2017; Leyns et al., 2017; Olah et al., 2018; Sobue et al., 2021). Based on the observation that signature microglial genes were downregulated at 4 h and 3 days, we suspected that the microglial gene expression signature after stroke shares many similarities with microglial reactivity in other disease and injury models. To identify specific features of the microglial stroke response which might be shared by other disease/injury states, we compared our datasets to lists of genes from published microglia gene expression datasets reflecting different inflammatory states (Table 1). These included microglial gene upregulation in response to LPS, aging, degenerative disease, *SOD1*<sup>G93A</sup> mutation, white matter injury, and traumatic brain injury (Bennett et al., 2016; Chiu et al., 2013; Hammond et al., 2019; Izzy et al., 2019; Keren-Shaul et al., 2017; Sousa et al., 2017). These datasets were selected because they represent mouse microglia gene signatures in both acute injury and degenerative disease states, and statistical information about their gene lists was publicly available. All gene sets, except white matter injury at 4 h, were significantly enriched in stroke-upregulated genes sets from

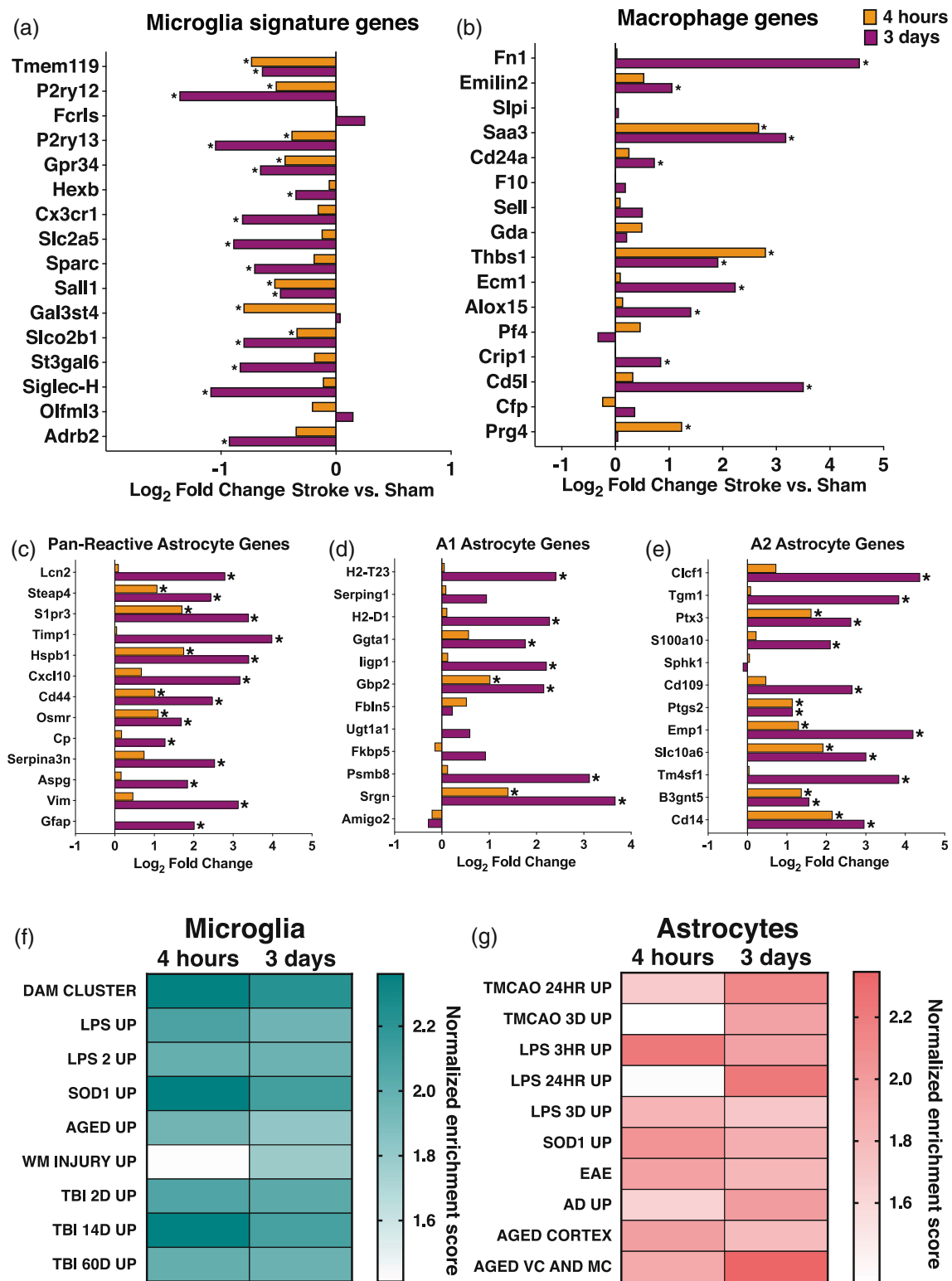


**FIGURE 6** Comparisons to other glial states and disease models. Log<sub>2</sub> fold change in microglial (a,b) and astrocyte (c–e) gene expression in stroke versus sham samples at 4 h and 3 days after dMCAO stroke for select microglial signature genes (a), select macrophage marker genes (b), pan-reactive astrocyte genes (c), A1 neurotoxic genes (d), and A2 neurotrophic genes (e). Gene set enrichment analysis results comparing microglial (f) and astrocyte (g) gene expression at 4 h and 3 days after stroke to published datasets of microglia and astrocyte reactivity in various disease and injury states. Darker color indicates higher normalized enrichment score for each comparison. All datasets were significantly enriched in respective post-stroke glial transcript lists from both timepoints, except white matter injury (WM Injury Up) and LPS after 24 h (LPS 24 h up), using an FDR <25%. Table 1 lists references for gene set sources. \*adj *p* < .05.

both timepoints (Figure 6F). Samples from the 4 h stroke group had greater enrichment in genes from the LPS, neurodegeneration, and traumatic brain injury sets. This was striking, since LPS and neurodegeneration are very different inflammatory states compared to an acute sterile tissue injury like ischemic stroke. We identified several genes, including *Spp1*, *Tlr2*, *Ccl3*, *H2-K1*, and *Ccl4*, which are upregulated in almost all of the inflammatory models analyzed and may comprise a core microglial inflammatory gene expression signature.

Similarly, we explored how generalizable the astrocytic stroke response was to other disease/injury states, choosing astrocyte-specific datasets for comparison from a variety of inflammatory contexts (Table 1). Diseased astrocyte gene sets were from tMCAO, LPS, SOD1<sup>G37R</sup> mutation, EAE, Alzheimer's disease, and aging (Boisvert et al., 2018; Borggrewe et al., 2021; Clarke et al., 2018; Hasel et al., 2021; Orre et al., 2014; Rakers et al., 2019; Sun et al., 2015; Zamanian et al., 2012). As with microglia, almost all diseased astrocyte gene sets were enriched in our astrocyte datasets from both 4 h and 3 days after stroke (Figure 6G). The only exception was astrocytes 24 h after LPS. Published gene sets from LPS 3 h and 3 days, SOD1, EAE, and aged cortex were slightly more enriched in our 4 h upregulated astrocyte genes versus 3 days. Highly expressed shared genes included *Cebpd* and *Junb* (LPS 3 h, SOD1, and EAE), *Cebpb* and *Gadd45g* (LPS 3 h and SOD1), and *Fos* (LPS 3 h and EAE). Interestingly, most of these genes are transcription factors known to induce the expression of pro-inflammatory genes. *Cebpb* and *Cebpd* promote the expression of IL-6, TNF $\alpha$ , and IL-1 $\beta$  (Akira et al., 1990; Pope et al., 1994; Shirakawa et al., 1993), and have been characterized as cortical astrocyte immediate-early genes after LPS (Cardinaux et al., 2000). The remaining gene sets (transient MCAO 24 h, transient MCAO 3 days, LPS 24 h, Alzheimer's disease, and aged motor and visual cortex) were more enriched in our 3 day stroke-upregulated astrocyte gene set. Shared genes between these datasets include known reactive astrocyte markers (*Vim*, *Gfap*, *Serpina3n*), and proliferation associated (*Efemp2*, *Spp1*), extracellular matrix remodeling (*Timp1*, *Ecm1*) anti-inflammatory (*Gpnb*, *Tmem176a*, *Tmem176b*), and pro-inflammatory genes (*Tnfrsf12a*, *Ctss*). Overall, the selected microglial gene sets were more enriched in the microglia 4 h versus 3 day post-stroke data, while the chosen astrocyte gene sets were evenly distributed between the two astrocyte timepoints.

### 3.7 | Enriched microglial and astrocyte processes and pathways at 4 h and 3 days after stroke

Gene ontology analysis revealed that top biological processes involving the genes significantly upregulated at 4 h after stroke in microglia included inflammatory response, response and regulation of IL-1, and transcription regulation (Figure 7A). Furthermore, strong pro-inflammatory pathways such as TNF signaling, NF- $\kappa$ B signaling, and Toll-like receptor signaling were highly upregulated (Figure 7B). In astrocytes at 4 h, half of the top biological processes were shared with the top processes in microglia: inflammatory response, immune response, response to lipopolysaccharide, positive regulation of tumor

necrosis factor production, and positive regulation of interleukin-1  $\beta$  production (Figure 7C). The remaining top processes were also related to a pro-inflammatory immune response. Astrocytes also shared many KEGG pathways in common with microglia at 4 h such as TNF, NF- $\kappa$ B, MAPK, and IL-17 signaling (Figure 7D).

At 3 days after stroke, different pathways were identified by gene ontology analysis in both cell types. In microglia, the top biological processes and pathways reflected a functional shift and were related to cell cycling and division (Figure 7e). Immune pathways and processes also remained upregulated, including virus response genes, and phagosome-related genes (Figure 7f). In contrast, astrocytes retain a highly inflammatory profile at 3 days with most top biological processes relating to inflammation and immunity (Figure 7g). Some of the top enriched KEGG pathways were related to cytokine and cytokine receptor interactions (Figure 7h), which were also enriched at 4 h in both cell types. However, the persistence of these pathways at 3 days could indicate that astrocytes rely more on cell-to-cell interactions at 3 days than microglia.

### 3.8 | Microglia initiate an early pro-inflammatory response through TNF signaling that may be propagated by astrocytes at 4 h after stroke

At 4 h after stroke, microglia and astrocytes shared a similar inflammatory profile, as indicated by high overlap of enriched KEGG and GO Biological Processes. This led us to interrogate how unique and shared genes in microglia and astrocytes at 4 h contribute to the acute immune response. Using the list of genes upregulated by stroke at 4 h in microglia (Figure 3a) and astrocytes (Figure 3b), we created a list of unique microglia genes (242 genes), unique astrocyte genes (233 genes), and shared genes by both cell types (100 genes). We performed KEGG pathway analysis on these three gene lists to obtain unique microglia (Figure 8a), unique astrocyte (Figure 8b), and shared (Figure 8c) KEGG pathways at 4 h after stroke. Signaling pathways such as apoptosis and AGE-RAGE were uniquely enriched in the top microglia KEGG pathways. In astrocytes, top unique pathways included complement cascade, cell adhesion, and leukocyte migration. The common shared pathways reflected many of the similarities observed using all upregulated genes at 4 h for each cell type (Figure 7b,d): TNF, IL-17, MAPK, and NF- $\kappa$ B signaling pathways.

One advantage of obtaining microglia and astrocyte-enriched transcriptomes at the same time points is the ability to examine how each cell contributes to pathways. After stroke, the TNF signaling pathway in both microglia and astrocytes has been found to disrupt blood brain barrier function and worsen outcomes (Chen et al., 2019; Li et al., 2022). Because it was enriched in all three gene lists and is important in pro-inflammatory signaling, we chose the KEGG TNF signaling pathway (Kanehisa & Goto, 2000) to highlight the ability of our data to identify unique microglial, astrocyte, and shared gene contributions. TNF itself was uniquely upregulated by microglia at 4 h after stroke (Figure 8d). All three downstream transcription factors (TFs) in the TNF pathway (AP-1, CREB, and C/EBP $\beta$ ) were upregulated by

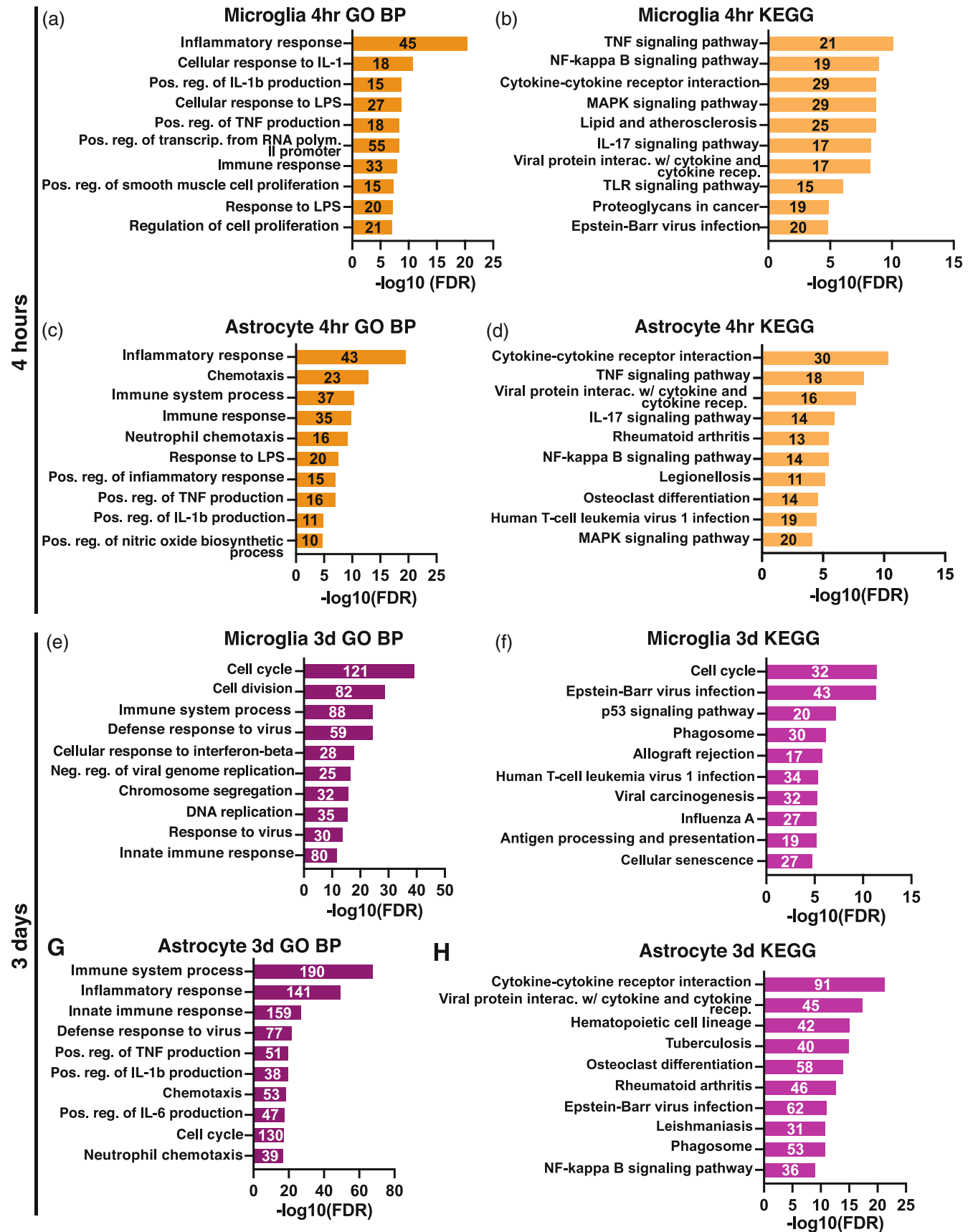


FIGURE 7 Legend on next page.

either or both cell types. These then modulate downstream target genes with distinct functions (right side of Figure 8d). For each functional category there were genes upregulated in either or both cell types, revealing differential regulation within astrocytes and microglia. Notably, leukocyte activation and vascular effects were uniquely upregulated by microglia, while pattern recognition receptors, cell adhesion, and remodeling of the extracellular matrix were uniquely upregulated by astrocytes.

### 3.9 | Microglia and astrocytes differentially regulate transcription at the hyperacute and acute period after stroke

To understand how astrocytes and microglia initiate and propagate inflammation, we used the transcription factors-target database TRRUST (Han et al., 2018) to identify transcription factors and their targets across time points. In the 4 h transcription factor-4 h target

relationships (Figure 9a,b), microglia had greater numbers of upregulated transcription factors (19), targets (36), and number of interactions (53) compared to astrocytes (11 transcription factors, 22 targets, 35 interactions). However, *Jun* (jun proto-oncogene, AP-1 transcription factor subunit) and *Egr1* (early growth response 1), were upregulated in both microglia and astrocytes, and together contributed to 37.7% and 45.7% respectively of the total number of interactions at 4 h.

We were also interested in how gene regulation in the hyperacute 4 h period could affect gene expression at the acute 3 day period (Figure 9c,d). Here we observed a shift to astrocytes expressing more transcription factors (18), targets (61), and interactions (90) compared to microglia (13 transcription factors, 23 targets, and 29 interactions). The targets of *Jun* and *Egr1* remain upregulated at 3 days, as demonstrated by *Jun* and *Egr1* contributing 41.4% and 36.7% of all transcription factor-target interactions in microglia and astrocytes respectively. In astrocytes, *Ets1* (ETS proto-oncogene 1, transcription factor) and *Sp1* (Spi1 proto-oncogene) also emerged as prominent drivers of upregulated targets.

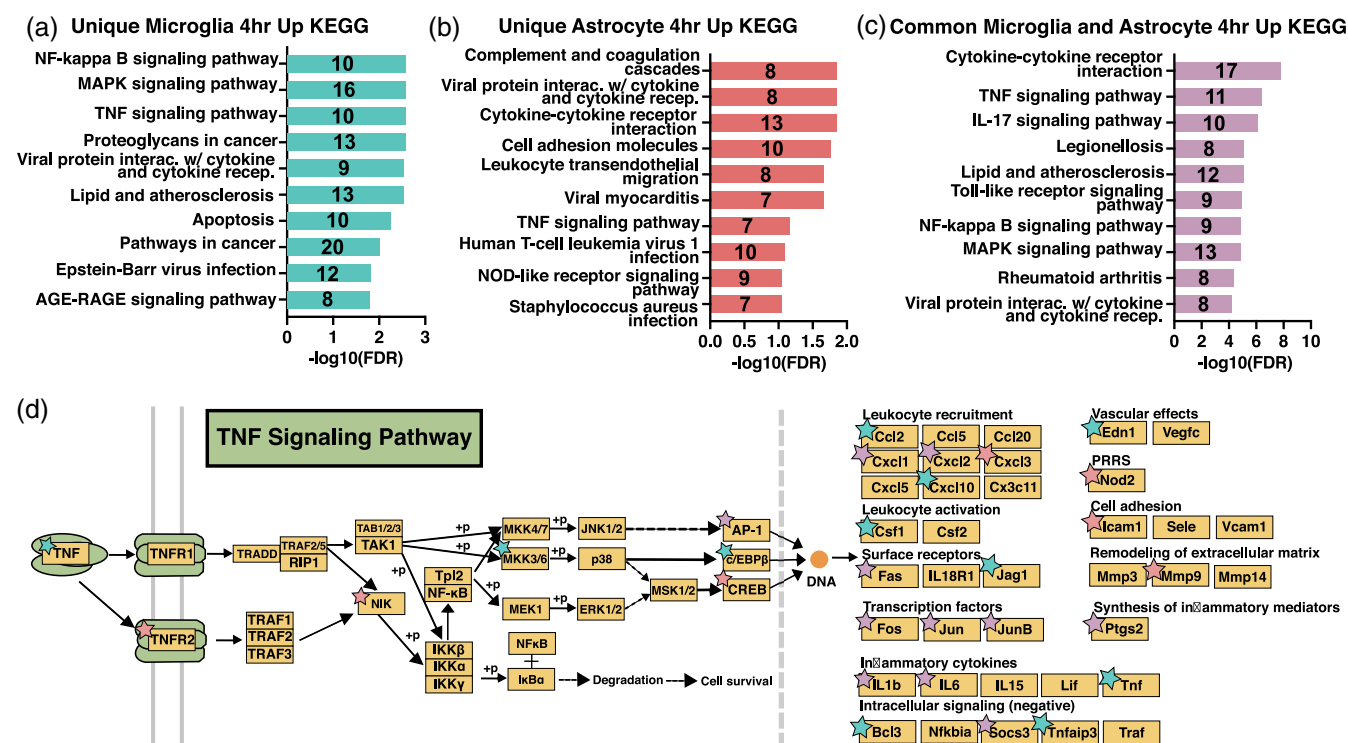


**FIGURE 8** Microglia initiate an early pro-inflammatory response through TNF signaling that is propagated by astrocytes at 4 h after stroke. KEGG pathways analysis results for genes upregulated 4 h after stroke and unique to microglia (a) or astrocytes (b), or common to both (c). GO terms are labeled on the y-axis, and the number of genes from each list found in the datasets are indicated on the respective bar in the plots. (d) KEGG TNF signaling pathway schematic, adapted from Kanehisa Laboratories (Kanehisa & Goto, 2000), with stars denoting unique enriched upregulated genes in microglia (blue), astrocytes (pink), and shared common (purple) at 4 h after stroke.

**FIGURE 7** Enriched microglial and astrocyte processes and pathways at 4 h and 3 days after stroke. Gene ontology analysis results for the top significantly enriched Biological Processes (left) and KEGG pathways (right) for microglia and astrocyte genes upregulated at 4 h (a–d) and 3 days (e–g) after stroke. GO terms are labeled on the y-axis, and the number of genes from each list found in the datasets are indicated on the respective bar in the plots.





Finally, we looked to see how upregulated transcription factors at 3 days relate to targets at 3 days (Figure 9e,f). The pattern of astrocytes expanding their transcription factor-target interactions continued with 41 transcription factors, 67 targets, and 99 interactions compared to the 12 transcription factors, 22 targets, and 28 interactions in microglia. *Stat1* (signal transducer and activator of transcription 1) emerged as the dominant TF in microglia, while *Spi1* continued as a top transcription factor in astrocytes. Interestingly, in all relationships except 3 day astrocyte transcription factor-target, the number of upregulated transcription factors remained below 20, with the number of targets largely contributing to changes in total interactions. However, in astrocytes at 3 days, the number of transcription factors greatly increases, with the average number of targets per transcription factor decreasing. Overall, we infer that microglia exhibit transcriptional regulation in response to stroke to a greater extent in the hyperacute period, while astrocytes use it in the acute period.

## 4 | DISCUSSION

We present a comprehensive molecular signature of hyperacute (4 h) and acute (3 days) transcriptional responses to stroke in microglia and astrocytes, two critical brain resident glial cell types for post-stroke neuroinflammation. To our knowledge, this is the first comprehensive characterization of microglial and astrocyte gene expression changes during the hyperacute period (4 h) after stroke. To improve the value of the data, we constructed a user-friendly website (<https://buckwalterlab.shinyapps.io/AstrocyteMicrogliaRiboTag/>) where researchers can easily look up gene changes.

We report that at 4 h after stroke, microglia and astrocytes upregulate genes characteristic of a distinctly pro-inflammatory response, including chemokines, heat shock proteins, transcription factors, and other signaling molecules which amplify inflammation. These results suggested that early after stroke, microglia are strongly proinflammatory and are particularly involved in activities such as propagation of inflammation and regulation of transcription. During the acute phase of neuroinflammation, microglia maintain a proinflammatory gene expression signature, but are strongly proliferative and entering a phagocytic state. In contrast, astrocytes appear to be similarly proinflammatory at 4 h, but rather than shift to a predominantly proliferative state like microglia, they remain in a proinflammatory state at 3 days. Despite astrocyte RiboTag group sizes being much larger than microglia RiboTag at 4 h (Methods 2.8), we observed a comparable number of differentially expressed genes in astrocytes and microglia at 4 h after stroke. In the top GO Biological Processes, 4 h and 3 day

astrocytes share 60% of processes, all related to inflammation. By comparison, 4 h and 3 day microglia did not share any top GO Biological Processes, indicating how the microglial profile drastically shifts while the astrocyte one maintains and strengthens an inflammatory signature.

Cumulatively, the gene expression changes we observed at 4 h after stroke suggest that microglia and astrocytes acutely respond to cerebral ischemia by turning on a distinct inflammatory gene expression program. Some of the most highly expressed and significantly upregulated genes in both cell types at this early time point were heat shock and stress response proteins, which may protect microglia and astrocytes by functioning as molecular chaperones during ischemic stress (Sun et al., 2006; van der Weerd et al., 2005; Yenari et al., 2008). The microglia specific profile at 4 h was composed of pro-inflammatory cytokines and chemokines, including *TNF $\alpha$* , *Ccl2*, *Ccl3*, *Ccl4*, and *Cxcl2*. Key functions of these molecules are positive regulation of the inflammatory response and recruitment of monocytes and neutrophils (Campbell et al., 2007; Mirabelli-Badenier et al., 2011; Wu et al., 2015). Therefore, it appears that one of the main functions of microglia early after stroke is to initiate the recruitment of peripheral immune cells into the damaged brain.

We report that there is a more similar canonical pro-inflammatory response in microglia during the hyperacute stroke response, rather than at 3 days. *Ccl3* and *Ccl4* were recently identified as markers of aged and neurodegeneration-associated microglia (Hammond et al., 2019; Kang et al., 2018), but the function of these chemokines in aging and neurodegeneration is unknown, and it is unclear if *Ccl3* and/or *Ccl4* signaling might have a unique role in the neuroinflammatory response after stroke. Our results reveal distinct microglial translational footprints at 4 h versus 3 days after ischemic stroke, but our analysis also highlights that many of the core genes upregulated at both time points after stroke are also upregulated by microglia in various other disease and inflammatory models.

Astrocytes also display common responses in multiple disease contexts, albeit to a lesser extent compared to microglia. *Gpnmb* was shared by the largest proportion of datasets (LPS 24 h, transient MCAO 24 h, transient MCAO 3 days, and aged motor and visual cortex), which spans from acute to chronic inflammatory states in the brain. *Gpnmb* has been found to attenuate neuroinflammation in vitro (Neal et al., 2018) via CD44 signaling, which is most highly expressed in our data at 3 days after stroke in astrocytes. While *Gpnmb* has largely been found to be anti-inflammatory in certain pathological conditions, there is also evidence of pro-inflammatory activity (Saade et al., 2021) in others, calling for the need for further exploration. Other shared genes, *Ctss* and *Spp1*, have both been found to disrupt

**FIGURE 9** Microglia and astrocytes differentially regulate transcription at the hyperacute and acute period after stroke. Circular lollipop plots illustrating upregulated transcription factors and their upregulated targets at 4 h and 3 days. Upregulated transcription factor-target relationships were analyzed for 4 h transcription factors and 4 h targets (a,b), 4 h transcription factors and 3 day targets (c,d), and 3 day transcription factors and 3 day targets (e,f). Inner wedges represent the upregulated transcription factors, while each line represents its upregulated target. Length of each line indicates the log<sub>2</sub> fold change of the target in stroke versus sham, while the size of the circle at the end of line indicates the transcripts per million of the target.



the blood brain barrier after stroke, with neutralization leading to improved outcomes (Wu et al., 2015; Spitzer et al., 2022; Xie et al., 2023). Our analysis comparing astrocyte gene expression after stroke to pan-reactive, A1, and A2 genes (Liddelw et al., 2017) serves as further motivation to stray away from strict classification of astrocytes as neurotoxic A1 or neurotrophic A2, as these findings demonstrate astrocytes express complex gene expression that is disease and time-dependent. However, we found key signature genes (*Steap4*, *S1pr3*, *Hspb1*, *Cd44*, *Osmr*) that may be used to mark pan-reactive astrocytes as early as 4 h after stroke and into the 3 day period. Overall, the astrocyte response at both time points shares some commonalities with other disease models, but also maintains a unique stroke signature that is time-dependent.

In addition to commonalities between disease states, microglia and astrocytes display commonalities to each other in stroke. There was a high overlap of top KEGG pathways enriched in upregulated genes in both cell types in the hyperacute period. This included the pro-inflammatory pathways IL-17, NF- $\kappa$ B, MAPK, TLR, and TNF signaling. The TNF signaling pathway was of particular interest given that activated microglia can induce reactive astrocytes by secreting TNF (Liddelw et al., 2017). In our data, microglia began expressing *Tnf* at 4 h after stroke, the initiator of the TNF signaling pathway, while astrocytes expressed downstream TNF pathway transcription factors such as *Fos*, *Jun*, and *Creb*. Thus, the two cell types may be working in concert to execute the TNF response. Also, while microglia have been established as immediate responders to injury by rapid migration to the site of tissue (Yoon et al., 2015), astrocytes also begin a unique injury response as early as 4 h after stroke. Pro-inflammatory factors such as TNF- $\alpha$  secreted from microglia may initiate the pro-inflammatory signaling pathway that astrocytes respond to through upregulation of transcription factors early on to ramp up their immune response at later time points.

Transcriptional differences were greater in both microglia and astrocytes compared to sham animals during the acute phase (3 days post-stroke) of neuroinflammation, versus the hyperacute phase (4 h post-stroke). This is not surprising, because inflammation approaches maximum levels at 3 days in the dMCAO stroke model (Chaney et al., 2019). Specific microglial gene expression changes at 3 days after stroke indicated a more complex response, and involved many genes associated with proliferation, phagocytosis, and sustained inflammation, suggesting that microglia continue to regulate neuroinflammation throughout the acute period after stroke. Microglia are less susceptible to ischemic damage than neurons and astrocytes, but studies indicate a loss of microglia in the ischemic region during the first 2 days after stroke, followed by gradual rebound in numbers over about a week (Liu et al., 2019; Ritzel et al., 2015). The proliferative transcriptional signature in our dataset likely reflects both a response to injury as well as this repopulation response.

By 3 days after stroke, astrocytes intensify the pro-inflammatory profile initiated at 4 h into a primarily immune-driven response. In the top 10 GO Biological Processes, seven were related to an immune or pro-inflammatory response. Specifically, genes associated with the

production of pro-inflammatory cytokines IL-1 $\beta$ , TNF- $\alpha$ , and IL-6 were upregulated. Compared to 4 h, stroke upregulated a greater number of transcription factors and their targets at 3 days in astrocytes after stroke. Of particular interest are transcription factors *C/EBP $\beta$* , *Spi1*, and *Rel*, which account for 25% of all upregulated transcription factor-target interactions and are each strong candidates as therapeutic targets. Absent or reduced *C/EBP $\beta$*  has been directly associated with smaller infarct sizes, diminished cognitive deficits, reduced inflammation after tMCAO (Kapadia et al., 2006), and increased angiogenesis after stroke (Li et al., 2020). *Spi1* has also been found to be upregulated in astrocytes 3 days after tMCAO (Rakers et al., 2019) and in bulk tissue after tMCAO (Stevens et al., 2011; Vartanian et al., 2011; Zhang et al., 2019), has been identified as a regulator of astrocytic wound responses (Burda et al., 2022), and can influence NF- $\kappa$ B signaling (Jin et al., 2011). Another member of the NF- $\kappa$ B signaling cascade, *Rel*, has been shown to play a role in hippocampus-dependent memory formation (Aleyasin et al., 2004; Levenson et al., 2004) and can confer cellular resistance to hypoxia (Qiu et al., 2001). Thus, *Rel* is a promising candidate for amelioration of post-stroke cognitive deficits. It may be that the initiation and persistence of these transcription factors are key for determining proper resolution of the immune response to stroke. Importantly, we report substantial differences between both cell types' gene expression during hyperacute versus acute neuroinflammation after stroke. Specifically, microglia respond rapidly by upregulating transcription factors and shift away from a purely pro-inflammatory state by 3 days after stroke, whereas astrocytes remain in a pro-inflammatory state across the acute phase.

Surprisingly, we found few sex-differences in the microglial and astrocyte response. Brain-wide changes in gene expression as well as neuroprotective capacity of microglia (Villa et al., 2018) and astrocyte reactivity (Cordeau et al., 2008) have been reported by others to be dependent on sex after stroke. In addition, there is clear data on sex-dependent differences in outcomes (Branyan & Sohrabji, 2020; Noh et al., 2023). There are also significant sex differences in adult microglial gene expression in wildtype mice (Guneykaya et al., 2018), under germ free conditions (Thion et al., 2018), after LPS stimulation (Hanamsagar et al., 2017), and in astrocyte gene expression in EAE (Tassoni et al., 2019), early development (Rurak et al., 2022), and in humans (Krawczyk et al., 2022). It may be that the gene differences we did observe in microglia may drive differences in stroke outcomes in females, or that these are less prominent in the dMCAO model because it does not model reperfusion. In addition, differences in the gene expression profiles reported by us compared to others may be due to differences in isolation techniques. It may be that microglial isolation by cell sorting skews gene expression towards a pro-inflammatory state and accounts for the higher representation of pro-inflammatory genes in other studies compared to ours (Haimon et al., 2018; Kang et al., 2018; Kronenberg et al., 2018; Rajan et al., 2019) or that sorting-based isolation may differentially affect gene expression in male versus female microglia. Data on sex differences in astrocyte gene expression is limited, but previous work that also used both sexes with a ribosomal pulldown method to isolate

astrocyte RNA after stroke reported no sex differences (Rakers et al., 2019). Furthermore, female and male group sizes were unbalanced in astrocytes at 4 h, which could have introduced a bias towards more differentially expressed genes in males. However, even fewer sex differences were observed in astrocytes compared to microglia at 4 h. This is an area which requires further investigation, but this implies that there are not significant sex differences in the astrocyte transcriptome after stroke.

Indeed, we chose the RiboTag method to avoid known gene changes from cell dissociation techniques that may confound stroke-induced changes particularly at the 4 h time point. The 4 h acute time point is critical because it is a clinically accessible time point for delivery of future therapies, and our data provides the first published resource describing it. The next earliest astrocyte and microglial transcriptomes after stroke were 12 h after stroke (Ma et al., 2022; Zheng et al., 2022). Other advantages of our study are the high number of biological replicates, use of both sexes, and high sequencing depth (>12 million reads per sample). Our data provide a starting point for identifying candidate pathways and signaling cascades that microglia and astrocytes may be using in a complementary fashion.

Our study has limitations. First, it solely reflects changes in 10–12 week old C57BL/6J mice after dMCAO stroke. Although there has been a rise in global stroke burden in young and middle-aged adults (Feigin et al., 2014), aged mice will need to be incorporated in future stroke transcriptomic studies. Interestingly, our gene set enrichment analysis demonstrated that our 3 day astrocyte DEGs were enriched in a healthy, aged astrocyte population (Boisvert et al., 2018). The dMCAO stroke model was selected for this study based on its recapitulation of cerebral ischemia-without-reperfusion in humans, its low mortality rate in mice and its ability to produce moderately-sized strokes in a consistent cortical location. However, this model does not model reperfusion injury which may respond differently to some neuroimmune therapies (Fluri et al., 2015; Llovera et al., 2015). Also, microglia and astrocytes were not sequenced from the same animals so direct statistical comparisons between the two cell types are not possible. There are also numerous reports of altered neuroinflammatory responses in fractalkine receptor knockout animals (Soriano et al., 2002; Tang et al., 2014) and our microglia RiboTag mice (Cx3cr1<sup>CreER2-IRES-eYFP/+</sup>;Rpl22<sup>HA+/+</sup>) are haploinsufficient for the fractalkine receptor. We did not detect changes in stroke size or gross microglia reactivity in our model, but more comprehensive methods, such as single cell RNAseq or utilization of a split Cre model (Kim et al., 2021) might detect more subtle effects of fractalkine receptor gene dose reduction. Finally, a limitation inherent to all RNAseq methods is the imperfect translation of RNA into protein. Compared to the mouse transcriptome, the transcriptome is more representative of the proteome (Wang et al., 2020). However, divergences between translating mRNA and functional protein can occur (Boutej et al., 2017) and it will be important to validate potential gene targets at the protein level. We observed high expression and cell-specificity of upregulated astrocyte and microglial genes of interest at 3 days after stroke (Figure S3). Future studies targeting the differentially

expressed genes outlined above will also need to confirm protein expression.

In summary, our results show that ischemic stroke induces substantial gene expression changes in microglia and astrocytes very early after injury that continue thereafter. Importantly, we found differences in the response profiles at each of these time points, supporting the concept that microglia and astrocytes play distinct roles in both initiation and regulation of neuroinflammation after stroke. Our data provide a useful resource for future studies investigating the functions of microglia and astrocytes in the response to ischemic stroke and may facilitate exploration of new targets for stroke treatments. For example, our analysis of the TNF pathway demonstrates the utility of this dataset in dissecting cell-specific responses to stroke. By examining gene changes in our user-friendly website (<https://buckwalterlab.shinyapps.io/AstrocyteMicrogliaRiboTag/>), we hope that stroke researchers will be able to generate hypotheses to speed our understanding of the neuroinflammatory response to stroke and develop therapies. Future work will also investigate how particular targets identified by our analysis affect stroke outcomes. Additionally, these experiments point to the usefulness of the RiboTag method for studying the time course of injury responses in the central nervous system.

#### ACKNOWLEDGMENTS

This work was funded by the National Institutes of Health R01NS067132 to MSB and T32MH020016 to VGH, American Heart Association/Allen Frontiers Group Brain Health Award 19PABH134580007 to MSB, Leducq Foundation Transatlantic Network of Excellence 19CVD01 to MSB, and Stanford Graduate Fellowship and Horatio Alger Dennis Washington Leadership Graduate Scholarship to VGH. VGH, KJL, TCP, LZ, TAL, KPB, JOO, and AID performed experiments and analyzed data. AJG assisted with study design and data analysis, and VGH, KJL, and MSB conceived of the study, designed the experiments, analyzed data and wrote the manuscript. We would like to acknowledge the Stanford Center for Genomics and Personalized Medicine, the Stanford Genomics Facility, the Stanford Shared FACS Facility for assistance with flow cytometry analysis, and the Stanford Protein and Nucleic Acid facility for processing RNAseq samples, for oligo synthesis, and for access to equipment. We would like to acknowledge Louis Andrews for coding assistance for data analysis, Kristy Zera and Elizabeth Mayne for their help with manuscript revisions, and Kanehisa Laboratories for granting copyright permission for the TNF signaling pathway.

#### CONFLICT OF INTEREST STATEMENT

The authors declare no conflict of interests.

#### DATA AVAILABILITY STATEMENT

Transcriptome datasets generated from microglia, astrocytes, and whole brain cortical mRNA can be accessed through GEO (Accession #GSE225110) as raw fastq files and processed count, TPM, and FPKM data. To improve visualization of the complete processed data set, a web application was developed; this can be found at <https://buckwalterlab.shinyapps.io/AstrocyteMicrogliaRiboTag/>.



## ORCID

- Victoria G. Hernandez <https://orcid.org/0000-0001-6740-1472>  
 Kendra J. Lechtenberg <https://orcid.org/0000-0002-3344-1289>  
 Todd C. Peterson <https://orcid.org/0000-0001-5441-6157>  
 Tawaun A. Lucas <https://orcid.org/0000-0002-2273-270X>  
 Karen P. Bradshaw <https://orcid.org/0000-0002-0338-7672>  
 Justice O. Owah <https://orcid.org/0000-0003-3402-4820>  
 Alanna I. Dorsey <https://orcid.org/0000-0001-6128-8050>  
 Andrew J. Gentles <https://orcid.org/0000-0002-0941-9858>  
 Marion S. Buckwalter <https://orcid.org/0000-0003-2807-2447>

## REFERENCES

- Akira, S., Isshiki, H., Sugita, T., Tanabe, O., Kinoshita, S., Nishio, Y., Nakajima, T., Hirano, T., & Kishimoto, T. (1990). A nuclear factor for IL-6 expression (NF-IL6) is a member of a C/EBP family. *The EMBO Journal*, *9*(6), 1897–1906.
- Aleyasin, H., Cregan, S. P., Iyirhiaro, G., O'Hare, M. J., Callaghan, S. M., Slack, R. S., & Park, D. S. (2004). Nuclear Factor-(kappa)B modulates the p53 response in neurons exposed to DNA damage. *The Journal of Neuroscience*, *24*(12), 2963–2973.
- Anderson, M. A., Burda, J. E., Ren, Y., Ao, Y., O'Shea, T. M., Kawaguchi, R., Coppola, G., Khakh, B. S., Deming, T. J., & Sofroniew, M. V. (2016). Astrocyte scar formation aids central nervous system axon regeneration. *Nature*, *532*(7598), 195–200.
- Anderson, M. A., O'Shea, T. M., Burda, J. E., Ao, Y., Barlately, S. L., Bernstein, A. M., Kim, J. H., James, N. D., Rogers, A., Kato, B., & Wollenberg, A. L. (2018). Required growth facilitators propel axon regeneration across complete spinal cord injury. *Nature*, *561*(7723), 396–400.
- Arbaizar-Roviroso, M., Pedragosa, J., Lozano, J. J., Casal, C., Pol, A., Gallizioli, M., & Planas, A. M. (2023). Aged lipid-laden microglia display impaired responses to stroke. *EMBO Molecular Medicine*, *15*(2), e17175.
- Behfar, Q., Ramirez Zuniga, A., & Martino-Adami, P. V. (2022). Aging, senescence, and dementia. *The Journal of Prevention of Alzheimer's Disease*, *9*(3), 523–531.
- Beilharz, E. J., Russo, V. C., Butler, G., Baker, N. L., Connor, B., Sirimanne, E. S., Dragunow, M., Werther, G. A., Gluckman, P. D., Williams, C. E., & Scheepens, A. (1998). Co-ordinated and cellular specific induction of the components of the IGF/IGFBP axis in the rat brain following hypoxic-ischemic injury. *Brain Research. Molecular Brain Research*, *59*(2), 119–134.
- Bennett, M. L., Chris Bennett, F., Liddelov, S. A., Ajami, B., Zamanian, J. L., Fernhoff, N. B., Mulinyawe, S. B., Bohlen, C. J., Adil, A., Tucker, A., & Weissman, I. L. (2016). New tools for studying microglia in the mouse and human CNS. *Proceedings of the National Academy of Sciences of the United States of America*, *113*(12), E1738–E1746.
- Bohlen, C. J., Chris Bennett, F., Tucker, A. F., Collins, H. Y., Mulinyawe, S. B., & Barres, B. A. (2017). Diverse requirements for microglial survival, specification, and function revealed by defined-medium cultures. *Neuron*, *94*(4), 759–773.
- Boisvert, M. M., Erikson, G. A., Shokhirev, M. N., & Allen, N. J. (2018). The aging astrocyte transcriptome from multiple regions of the mouse brain. *Cell Reports*, *22*(1), 269–285.
- Borggrewe, M., Grit, C., Vainchtein, I. D., Brouwer, N., Wesseling, E. M., Laman, J. D., Eggen, B. J. L., Kooistra, S. M., & Boddeke, E. W. G. M. (2021). Regionally diverse astrocyte subtypes and their heterogeneous response to EAE. *Glia*, *69*(5), 1140–1154.
- Böttcher, J. P., Beyer, M., Meissner, F., Abdullah, Z., Sander, J., Höchst, B., Eickhoff, S., Rieckmann, J. C., Russo, C., Bauer, T., & Flecken, T. (2015). Functional classification of memory CD8(+) T cells by CX3CR1 expression. *Nature Communications*, *6*, 8306.
- Boutej, H., Rahimian, R., Thammisetty, S. S., Béland, L.-C., Lalancette-Hébert, M., & Kriz, J. (2017). Diverging mRNA and protein networks in activated microglia reveal SRSF3 suppresses translation of highly upregulated innate immune transcripts. *Cell Reports*, *21*(11), 3220–3233.
- Brnayan, T. E., & Sohrabji, F. (2020). Sex differences in stroke co-morbidities. *Experimental Neurology*, *332*, 113384.
- Burda, J. E., O'Shea, T. M., Ao, Y., Suresh, K. B., Wang, S., Bernstein, A. M., Chandra, A., Deverasetty, S., Kawaguchi, R., Kim, J. H., & McCallum, S. (2022). Divergent transcriptional regulation of astrocyte reactivity across disorders. *Nature*, *606*(7914), 557–564.
- Butovsky, O., Jedrychowski, M. P., Moore, C. S., Cialic, R., Lanser, A. J., Gabrieli, G., Koeglsperger, T., Dake, B., Wu, P. M., Doykan, C. E., & Fanek, Z. (2014). Identification of a unique TGF- $\beta$ -dependent molecular and functional signature in microglia. *Nature Neuroscience*, *17*(1), 131–143.
- Buttgereit, A., Lelios, I., Xueyang, Y., Vrohings, M., Krakoski, N. R., Gautier, E. L., Nishinakamura, R., Becher, B., & Greter, M. (2016). Sall1 is a transcriptional regulator defining microglia identity and function. *Nature Immunology*, *17*(12), 1397–1406.
- Campbell, S. J., Carare-Nnadi, R. O., Losey, P. H., & Anthony, D. C. (2007). Loss of the atypical inflammatory response in juvenile and aged rats. *Neuropathology and Applied Neurobiology*, *33*(1), 108–120.
- Cardinaux, J.-R., Allaman, I., & Magistretti, P. J. (2000). Pro-inflammatory cytokines induce the transcription factors C/EBP $\beta$  and C/EBP $\delta$  in astrocytes. *Glia*, *29*(1), 91–97.
- Chaney, A., Cropper, H. C., Johnson, E. M., Lechtenberg, K. J., Peterson, T. C., Stevens, M. Y., Buckwalter, M. S., & James, M. L. (2019). 11C-DPA-713 versus 18F-GE-180: A preclinical comparison of translocator protein 18 kDa PET tracers to visualize acute and chronic neuroinflammation in a mouse model of ischemic stroke. *Journal of Nuclear Medicine: Official Publication, Society of Nuclear Medicine*, *60*(1), 122–128.
- Chelluboina, B., Klopfenstein, J. D., Pinson, D. M., Wang, D. Z., Vemuganti, R., & Veeravalli, K. K. (2015). Matrix metalloproteinase-12 induces blood-brain barrier damage after focal cerebral ischemia. *Stroke: A Journal of Cerebral Circulation*, *46*(12), 3523–3531.
- Chen, A.-Q., Fang, Z., Chen, X.-L., Yang, S., Zhou, Y.-F., Mao, L., Xia, Y.-P., Jin, H. J., Li, Y. N., You, M. F., & Wang, X. X. (2019). Microglia-derived TNF- $\alpha$  mediates endothelial necroptosis aggravating blood brain-barrier disruption after ischemic stroke. *Cell Death & Disease*, *10*(7), 487.
- Chiu, I. M., Morimoto, E. T. A., Goodarzi, H., Liao, J. T., O'Keeffe, S., Phatnani, H. P., Muratet, M., Carroll, M. C., Levy, S., Tavazoie, S., & Myers, R. M. (2013). A neurodegeneration-specific gene-expression signature of acutely isolated microglia from an amyotrophic lateral sclerosis mouse model. *Cell Reports*, *4*(2), 385–401.
- Clarke, L. E., Liddelov, S. A., Chakraborty, C., Münch, A. E., Heiman, M., & Barres, B. A. (2018). Normal aging induces A1-like astrocyte reactivity. *Proceedings of the National Academy of Sciences of the United States of America*, *115*(8), E1896–E1905.
- Cordeau, P., Jr, M. L.-H., Weng, Y. C., & Kriz, J. (2008). Live imaging of neuroinflammation reveals sex and estrogen effects on astrocyte response to ischemic injury. *Stroke: A Journal of Cerebral Circulation*, *39*(3), 935–942.
- Dobin, A., Davis, C. A., Schlesinger, F., Drenkow, J., Zaleski, C., Jha, S., Batut, P., Chaisson, M., & Gingeras, T. R. (2013). STAR: Ultrafast universal RNA-Seq aligner. *Bioinformatics*, *29*(1), 15–21.
- Doyle, K. P., Fathali, N., Siddiqui, M. R., & Buckwalter, M. S. (2012). Distal hypoxic stroke: A new mouse model of stroke with high throughput, low variability and a quantifiable functional deficit. *Journal of Neuroscience Methods*, *207*(1), 31–40.
- Faulkner, J. R., Herrmann, J. E., Woo, M. J., Tansey, K. E., Doan, N. B., & Sofroniew, M. V. (2004). Reactive astrocytes protect tissue and preserve function after spinal cord injury. *The Journal of Neuroscience: The Official Journal of the Society for Neuroscience*, *24*(9), 2143–2155.

- Feigin, V. L., Forouzanfar, M. H., Krishnamurthi, R., Mensah, G. A., Connor, M., Bennett, D. A., Moran, A. E., Sacco, R. L., Anderson, L., Truelsen, T., & O'Donnell, M. (2014). Global and regional burden of stroke during 1990-2010: Findings from the Global Burden of Disease Study 2010. *The Lancet*, 383(9913), 245–254.
- Fluri, F., Schuhmann, M. K., & Kleinschnitz, C. (2015). Animal models of ischemic stroke and their application in clinical research. *Drug Design, Development and Therapy*, 9, 3445–3454.
- Gu, B. J., Huang, X., Amber, O., Rembach, A., Fowler, C., Avula, P. K., Horton, A., Doecke, J. D., Villemagne, V. L., Macaulay, S. L., & Maruff, P. (2016). Innate phagocytosis by peripheral blood monocytes is altered in Alzheimer's disease. *Acta Neuropathologica*, 132(3), 377–389.
- Guneykaya, D., Ivanov, A., Hernandez, D. P., Haage, V., Wojtas, B., Meyer, N., Maricos, M., Jordan, P., Buonfiglioli, A., Gielniewski, B., & Ochocka, N. (2018). Transcriptional and translational differences of microglia from male and female brains. *Cell Reports*, 24(10), 2773–2783.
- Haimon, Z., Volaski, A., Orthgiess, J., Boura-Halfon, S., Varol, D., Shemer, A., Yona, S., Zuckerman, B., David, E., Chappell-Maor, L., & Bechmann, I. (2018). Re-evaluating microglia expression profiles using ribotag and cell isolation strategies. *Nature Immunology*, 19(6), 636–644.
- Hammarberg, H., Risling, M., Hökfelt, T., Cullheim, S., & Piehl, F. (1998). Expression of insulin-like growth factors and corresponding binding proteins (IGFBP 1-6) in rat spinal cord and peripheral nerve after axonal injuries. *The Journal of Comparative Neurology*, 400(1), 57–72.
- Hammond, T. R., Dufort, C., Dissing-Olesen, L., Giera, S., Young, A., Wysoker, A., Walker, A. J., Gergits, F., Segel, M., Nemes, J., & Marsh, S. E. (2019). Single-cell RNA sequencing of microglia throughout the mouse lifespan and in the injured brain reveals complex cell-state changes. *Immunity*, 50(1), 253–271.
- Han, H., Cho, J.-W., Lee, S., Yun, A., Kim, H., Bae, D., Yang, S., Kim, C. Y., Lee, M., Kim, E., & Lee, S. (2018). TRRUST v2: An expanded reference database of human and mouse transcriptional regulatory interactions. *Nucleic Acids Research*, 46, D380–D386.
- Hanamsagar, R., Alter, M. D., Block, C. S., Sullivan, H., Bolton, J. L., & Bilbo, S. D. (2017). Generation of a microglial developmental index in mice and in humans reveals a sex difference in maturation and immune reactivity. *Glia*, 65(9), 1504–1520.
- Hasel, P., Rose, I. V. L., Sadick, J. S., Kim, R. D., & Liddelow, S. A. (2021). Neuroinflammatory astrocyte subtypes in the mouse brain. *Nature Neuroscience*, 24(10), 1475–1487.
- Hickman, S. E., Kingery, N. D., Ohsumi, T. K., Borowsky, M. L., Wang, L.-C., Means, T. K., & El Khoury, J. (2013). The microglial sensome revealed by direct RNA sequencing. *Nature Neuroscience*, 16(12), 1896–1905.
- Huang, D. W., Sherman, B. T., & Lempicki, R. A. (2009a). Systematic and integrative analysis of large gene lists using DAVID bioinformatics resources. *Nature Protocols*, 4(1), 44–57.
- Huang, D. W., Sherman, B. T., & Lempicki, R. A. (2009b). Bioinformatics enrichment tools: Paths toward the comprehensive functional analysis of large gene lists. *Nucleic Acids Research*, 37(1), 1–13.
- Iadecola, C., & Anrather, J. (2011). The immunology of stroke: From mechanisms to translation. *Nature Medicine*, 17(7), 796–808.
- Iadecola, C., Buckwalter, M. S., & Anrather, J. (2020). Immune responses to stroke: Mechanisms, modulation, and therapeutic potential. *The Journal of Clinical Investigation*, 130(6), 2777–2788.
- Izzy, S., Liu, Q., Fang, Z., Lule, S., Limin, W., Chung, J. Y., Sarro-Schwartz, A., Brown-Whalen, A., Perner, C., Hickman, S. E., & Kaplan, D. L. (2019). Time-dependent changes in microglia transcriptional networks following traumatic brain injury. *Frontiers in Cellular Neuroscience*, 13, 307.
- Jin, F., Li, Y., Ren, B., & Natarajan, R. (2011). PU.1 and C/EBP $\alpha$  synergistically program distinct response to NF- $\kappa$ B activation through establishing monocyte specific enhancers. *Proceedings of the National Academy of Sciences*, 108(13), 5290–5295.
- Jordão, M. J., Costa, R. S., Brendecke, S. M., Sagar, G. L., Tai, Y.-H., Tay, T. L., Schramm, E., Armbruster, S., Hagemeyer, N., & Groß, O. (2019). Single-cell profiling identifies myeloid cell subsets with distinct fates during neuroinflammation. *Science*, 363(6425), eaat7554.
- Kanehisa, M., & Goto, S. (2000). KEGG: Kyoto encyclopedia of genes and genomes. *Nucleic Acids Research*, 28(1), 27–30.
- Kang, S. S., Ebbert, M. T. W., Baker, K. E., Cook, C., Wang, X., Sens, J. P., Kocher, J.-P., Petrucelli, L., & Fryer, J. D. (2018). Microglial translational profiling reveals a convergent APOE pathway from aging, amyloid, and tau. *The Journal of Experimental Medicine*, 215(9), 2235–2245.
- Kapadia, R., Tureyen, K., Bowen, K. K., Kalluri, H., Johnson, P. F., & Vemuganti, R. (2006). Decreased brain damage and curtailed inflammation in transcription factor CCAAT/enhancer binding protein beta knockout mice following transient focal cerebral ischemia. *Journal of Neurochemistry*, 98(6), 1718–1731.
- Keren-Shaul, H., Spinrad, A., Weiner, A., Matcovitch-Natan, O., Dvir-Szternfeld, R., Ulland, T. K., David, E., Baruch, K., Lara-Astaiso, D., Toth, B., & Itzkovitz, S. (2017). A unique microglia type associated with restricting development of Alzheimer's disease. *Cell*, 169(7), 1276–1290.
- Khatchadourian, A., Bourque, S. D., Richard, V. R., Titorenko, V. I., & Maysinger, D. (2012). Dynamics and regulation of lipid droplet formation in lipopolysaccharide (LPS)-stimulated microglia. *Biochimica et Biophysica Acta*, 1821(4), 607–617.
- Kim, J. Y., Barua, S., Huang, M. Y., Park, J., Yenari, M. A., & Lee, J. E. (2020). Heat shock protein 70 (HSP70) induction: Chaperonotherapy for neuroprotection after brain injury. *Cells*, 9(9), 2020.
- Kim, J.-S., Kolesnikov, M., Peled-Hajaj, S., Scheyltjens, I., Xia, Y., Trzebanski, S., Haimon, Z., Shemer, A., Lubart, A., Van Hove, H., & Chappell-Maor, L. (2021). A binary Cre transgenic approach dissects microglia and CNS border-associated macrophages. *Immunity*, 54(1), 176–190.
- Krasemann, S., Madore, C., Cialic, R., Baufeld, C., Calcagno, N., El Fatimy, R., Beckers, L., O'loughlin, E., Xu, Y., Fanek, Z., & Greco, D. J. (2017). The TREM2-APOE pathway drives the transcriptional phenotype of dysfunctional microglia in neurodegenerative diseases. *Immunity*, 47(3), 566–581.
- Krawczyk, M. C., Haney, J. R., Pan, L., Caneda, C., Khankan, R. R., Reyes, S. D., Chang, J. W., Morselli, M., Vinters, H. V., Wang, A. C., & Cobos, I. (2022). Human astrocytes exhibit tumor microenvironment-, age-, and sex-related transcriptomic signatures. *The Journal of Neuroscience*, 42(8), 1587–1603.
- Kronenberg, G., Uhlemann, R., Richter, N., Klempin, F., Wegner, S., Staerck, L., Wolf, S., Uckert, W., Kettenmann, H., Endres, M., & Gertz, K. (2018). Distinguishing features of microglia- and monocyte-derived macrophages after stroke. *Acta Neuropathologica*, 135(4), 551–568.
- Lalancette-Hébert, M., Gowing, G., Simard, A., Weng, Y. C., & Kriz, J. (2007). Selective ablation of proliferating microglial cells exacerbates ischemic injury in the brain. *The Journal of Neuroscience*, 27(10), 2596–2605.
- Levenson, J. M., Choi, S., Lee, S.-Y., Cao, Y. A., Ahn, H. J., Worley, K. C., Pizzi, M., Liou, H.-C., & David Sweatt, J. (2004). A bioinformatics analysis of memory consolidation reveals involvement of the transcription factor c-Rel. *The Journal of Neuroscience*, 24(16), 3933–3943.
- Leyns, C. E. G., Ulrich, J. D., Finn, M. B., Stewart, F. R., Koscal, L. J., Serrano, J. R., Robinson, G. O., Anderson, E., Colonna, M., & Holtzman, D. M. (2017). TREM2 deficiency attenuates neuroinflammation and protects against neurodegeneration in a mouse model of tauopathy. *Proceedings of the National Academy of Sciences of the United States of America*, 114(43), 11524–11529.
- Li, B., & Dewey, C. N. (2011). RSEM: Accurate transcript quantification from RNA-Seq data with or without a reference genome. *BMC Bioinformatics*, 12, 323.



- Li, J., Lv, H., & Che, Y. (2020). microRNA-381-3p confers protection against ischemic stroke through promoting angiogenesis and inhibiting inflammation by suppressing Cebpb and Map3k8. *Cellular and Molecular Neurobiology*, 40(8), 1307–1319.
- Li, W., Liu, D., Jiaqi, X., Zha, J., Wang, C., An, J., Xie, Z., & Qiao, S. (2022). Astrocyte-derived TNF- $\alpha$ -activated platelets promote cerebral ischemia/reperfusion injury by regulating the RIP1/RIP3/AKT signaling pathway. *Molecular Neurobiology*, 59(9), 5734–5749.
- Liddelow, S. A., Guttenplan, K. A., Clarke, L. E., Bennett, F. C., Bohlen, C. J., Schirmer, L., Bennett, M. L., Münch, A. E., Chung, W. S., Peterson, T. C., & Wilton, D. K. (2017). Neurotoxic reactive astrocytes are induced by activated microglia. *Nature*, 541(7638), 481–487.
- Liu, Q., Johnson, E. M., Lam, R. K., Wang, Q., Ye, H. B., Wilson, E. N., Minhas, P. S., Liu, L., Swarovski, M. S., Tran, S., & Wang, J. (2019). Peripheral TREM1 responses to brain and intestinal immunogens amplify stroke severity. *Nature Immunology*, 20(8), 1023–1034.
- Llovera, G., Hofmann, K., Roth, S., Salas-Pédomo, A., Ferrer-Ferrer, M., Perego, C., Zanier, E. R., Mamrak, U., Rex, A., Party, H., & Agin, V. (2015). Results of a preclinical randomized controlled multicenter trial (pRCT): anti-CD49d treatment for acute brain ischemia. *Science Translational Medicine*, 7(299), 299ra121.
- Loix, M., Wouters, E., Vanherle, S., Dehairs, J., McManaman, J. L., Kemps, H., Swinnen, J. V., Haidar, M., Bogie, J. F. J., & Hendriks, J. J. A. (2022). Perilipin-2 limits remyelination by preventing lipid droplet degradation. *Cellular and Molecular Life Sciences: CMLS*, 79(10), 515.
- Love, M. I., Huber, W., & Anders, S. (2014). Moderated estimation of fold change and dispersion for RNA-Seq data with DESeq2. *Genome Biology*, 15(12), 550.
- Ma, H., Zhou, Y., Li, Z., Zhu, L., Li, H., Zhang, G., Wang, J., Gong, H., Xu, D., Hua, W., & Liu, P. (2022). Single-cell RNA-sequencing analyses revealed heterogeneity and dynamic changes of metabolic pathways in astrocytes at the acute phase of ischemic stroke. *Oxidative Medicine and Cellular Longevity*, 2022, 1817721.
- Marschallinger, J., Iram, T., Zardeneta, M., Lee, S. E., Lehallier, B., Haney, M. S., Pluvinage, J. V., Mathur, V., Hahn, O., Morgens, D. W., & Kim, J. (2020). Lipid-droplet-accumulating microglia represent a dysfunctional and proinflammatory state in the aging brain. *Nature Neuroscience*, 23(2), 194–208.
- Martin, M. (2011). Cutadapt removes adapter sequences from high-throughput sequencing reads. *EMBnet journal*, 17(1), 10–12.
- Mionnet, C., Buatois, V., Kanda, A., Milcent, V., Fleury, S., Lair, D., Langelot, M., Lacoëuille, Y., Hessel, E., Coffman, R., & Magnan, A. (2010). CX3CR1 is required for airway inflammation by promoting T helper cell survival and maintenance in inflamed lung. *Nature Medicine*, 16(11), 1305–1312.
- Mirabelli-Badenier, M., Braunersreuther, V., Viviani, G. L., Dallegrì, F., Quercioli, A., Veneselli, E., Mach, F., & Montecucco, F. (2011). CC and CXC chemokines are pivotal mediators of cerebral injury in ischaemic stroke. *Thrombosis and Haemostasis*, 105(3), 409–420.
- Mootha, V. K., Lindgren, C. M., Eriksson, K.-F., Subramanian, A., Sihag, S., Lehar, J., Puigserver, P., Carlsson, E., Ridderstråle, M., Laurila, E., & Houstis, N. (2003). PGC-1 $\alpha$ -responsive genes involved in oxidative phosphorylation are coordinately downregulated in human diabetes. *Nature Genetics*, 34(3), 267–273.
- Moretti, A., Ferrari, F., & Villa, R. F. (2015). Neuroprotection for ischaemic stroke: Current status and challenges. *Pharmacology & Therapeutics*, 146, 23–34.
- Neal, M. L., Boyle, A. M., Budge, K. M., Safadi, F. F., & Richardson, J. R. (2018). The glycoprotein GPNMB attenuates astrocyte inflammatory responses through the CD44 receptor. *Journal of Neuroinflammation*, 15(1), 73.
- Noh, B., McCullough, L. D., & Moruno-Manchon, J. F. (2023). Sex-biased autophagy as a potential mechanism mediating sex differences in ischemic stroke outcome. *Neural Regeneration Research*, 18(1), 31–37.
- Olah, M., Patrick, E., Villani, A.-C., Jishu, X., White, C. C., Ryan, K. J., Piehowski, P., Kapasi, A., Nejad, P., Cimpean, M., & Connor, S. (2018). A transcriptomic atlas of aged human microglia. *Nature Communications*, 9(1), 539.
- Orre, M., Kamphuis, W., Osborn, L. M., Melief, J., Kooijman, L., Huitinga, I., Klooster, J., Bossers, K., & Hol, E. M. (2014). Acute isolation and transcriptome characterization of cortical astrocytes and microglia from young and aged mice. *Neurobiology of Aging*, 35(1), 1–14.
- Papassotiropoulos, A., Fountoulakis, M., Duncley, T., Stephan, D. A., & Reiman, E. M. (2006). Genetics, transcriptomics, and proteomics of Alzheimers disease. *The Journal of Clinical Psychiatry*, 67(4), 652–670.
- Parkhurst, C. N., Yang, G., Ninan, I., Savas, J. N., Yates 3rd, J. R., Lafaille, J. J., Hempstead, B. L., Littman, D. R., & Gan, W.-B. (2013). Microglia promote learning-dependent synapse formation through brain-derived neurotrophic factor. *Cell*, 155(7), 1596–1609.
- Picelli, S., Faridani, O. R., Björklund, Å. K., Winberg, G., Sagasser, S., & Sandberg, R. (2014). Full-length RNA-seq from single cells using Smart-seq2. *Nature Protocols*, 9(1), 171–181.
- Pope, R. M., Leutz, A., & Ness, S. A. (1994). C/EBP beta regulation of the tumor necrosis factor alpha gene. *The Journal of Clinical Investigation*, 94(4), 1449–1455.
- Qiu, J., Grafe, M. R., Schmura, S. M., Glasgow, J. N., Kent, T. A., Rassin, D. K., & Perez-Polo, J. R. (2001). Differential NF-kappa B regulation of Bcl-X gene expression in hippocampus and basal forebrain in response to hypoxia. *Journal of Neuroscience Research*, 64(3), 223–234.
- Rahimian, R., Béland, L.-C., & Kriz, J. (2018). Galectin-3: Mediator of microglia responses in injured brain. *Drug Discovery Today*, 23(2), 375–381.
- Rajan, W. D., Wojtas, B., Gielniewski, B., Gieryng, A., Zawadzka, M., & Kaminska, B. (2019). Dissecting functional phenotypes of microglia and macrophages in the rat brain after transient cerebral ischemia. *Glia*, 67(2), 232–245.
- Rakers, C., Schleif, M., Blank, N., Matušková, H., Ulas, T., Händler, K., Torres, S. V., Schumacher, T., Tai, K., Schultze, J. L., & Jackson, W. S. (2019). Stroke target identification guided by astrocyte transcriptome analysis. *Glia*, 67(4), 619–633.
- Ritzel, R. M., Patel, A. R., Grenier, J. M., Crapser, J., Verma, R., Jellison, E. R., & McCullough, L. D. (2015). Functional differences between microglia and monocytes after ischemic stroke. *Journal of Neuroinflammation*, 12, 106.
- Rurak, G. M., Simard, S., Freitas-Andrade, M., Lacoste, B., Charif, F., Van Geel, A., Stead, J., Woodside, B., Green, J. R., Coppola, G., & Salmaso, N. (2022). Sex differences in developmental patterns of neo-cortical astrogliosis: A mouse transcriptome database. *Cell Reports*, 38(5), 110310.
- Saade, M., Araujo de Souza, G., Scavone, C., & Kinoshita, P. F. (2021). The Role of GPNMB in Inflammation. *Frontiers in Immunology*, 12:674739.
- Sanz, E., Yang, L., Thomas, S., Morris, D. R., Stanley McKnight, G., & Amieux, P. S. (2009). Cell-type-specific isolation of ribosome-associated mRNA from complex tissues. *Proceedings of the National Academy of Sciences of the United States of America*, 106(33), 13939–13944.
- Shichita, T., Ito, M., Morita, R., Komai, K., Noguchi, Y., Ooboshi, H., Koshida, R., Takahashi, S., Kodama, T., & Yoshimura, A. (2017). MAFB prevents excess inflammation after ischemic stroke by accelerating clearance of damage signals through MSR1. *Nature Medicine*, 23(6), 723–732.
- Shin, Y.-J., Kim, H. L., Choi, J.-S., Choi, J.-Y., Cha, J.-H., & Lee, M.-Y. (2011). Osteopontin: correlation with phagocytosis by brain macrophages in a rat model of stroke. *Glia*, 59(3), 413–423.
- Shirakawa, F., Saito, K., Bonagura, C. A., Galson, D. L., Fenton, M. J., Webb, A. C., & Auron, P. E. (1993). The human prointerleukin 1 beta gene requires DNA sequences both proximal and distal to the transcription start site for tissue-specific induction. *Molecular and Cellular Biology*, 13(3), 1332–1344.
- Simats, A., Ramiro, L., García-Berrococo, T., Briansó, F., Gonzalo, R., Martín, L., Sabé, A., Gill, N., Penalba, A., Colomé, N., & Sánchez, A.

- (2020). A Mouse brain-based multi-omics integrative approach reveals potential blood biomarkers for ischemic stroke. *Molecular & Cellular Proteomics*, 19(12), 1921–1936.
- Sobue, A., Komine, O., Hara, Y., Endo, F., Mizoguchi, H., Watanabe, S., Murayama, S., Saito, T., Saido, T. C., Sahara, N., & Higuchi, M. (2021). Microglial gene signature reveals loss of homeostatic microglia associated with neurodegeneration of Alzheimer's disease. *Acta Neuropathologica Communications*, 9(1), 1.
- Soriano, S. G., Amaravadi, L. S., Wang, Y. F., Zhou, H., Yu, G. X., Tonra, J. R., Fairchild-Huntress, V., Fang, Q., Dunmore, J. H., Huszar, D., & Pan, Y. (2002). Mice deficient in fractalkine are less susceptible to cerebral ischemia-reperfusion injury. *Journal of Neuroimmunology*, 125(1–2), 59–65.
- Sousa, C., Biber, K., & Michelucci, A. (2017). Cellular and molecular characterization of microglia: A unique immune cell population. *Frontiers in Immunology*, 8, 198.
- Spitzer, D., Guérit, S., Puetz, T., Khel, M. I., Armbrust, M., Dunst, M., Macas, J., Zinke, J., Devraj, G., Jia, X., Croll, F., Sommer, K., Filipski, K., Freiman, T. M., Looso, M., Günther, S., Di Tacchio, M., Plate, K.-H., Reiss, Y., & Devraj, K. (2022). Profiling the neurovascular unit unveils detrimental effects of osteopontin on the blood-brain barrier in acute ischemic stroke. *Acta Neuropathologica*, 144(2), 305–337.
- Srinivasan, R., Tsai-Yi, L., Chai, H., Ji, X., Huang, B. S., Golshani, P., Coppola, G., & Khakh, B. S. (2016). New transgenic mouse lines for selectively targeting astrocytes and studying calcium signals in astrocyte processes in situ and in vivo. *Neuron*, 92(6), 1181–1195.
- Steffen, J., Julio, A., Petra, G., Jean, S. M., Kreutzberg, G. W., Alan, S., & Littman, D. R. (2000). Analysis of fractalkine receptor CX3CR1 function by targeted deletion and green fluorescent protein reporter gene insertion. *Molecular and Cellular Biology*, 20(11), 4106–4114.
- Stevens, S. L., Leung, P. Y., Vartanian, K. B., Gopalan, B., Yang, T., Simon, R. P., & Stenzel-Poore, M. P. (2011). Multiple preconditioning paradigms converge on interferon regulatory factor-dependent signaling to promote tolerance to ischemic brain injury. *The Journal of Neuroscience*, 31(23), 8456–8463.
- Stuckey, S. M., Ong, L. K., Collins-Praino, L. E., & Turner, R. J. (2021). Neuroinflammation as a key driver of secondary neurodegeneration following stroke? *International Journal of Molecular Sciences*, 22(23), 13101.
- Subramanian, A., Tamayo, P., Mootha, V. K., Mukherjee, S., Ebert, B. L., Gillette, M. A., Paulovich, A., Pomeroy, S. L., Golub, T. R., Lander, E. S., & Mesirov, J. P. (2005). Gene set enrichment analysis: A knowledge-based approach for interpreting genome-wide expression profiles. *Proceedings of the National Academy of Sciences of the United States of America*, 102(43), 15545–15550.
- Sun, S., Sun, Y., Ling, S.-C., Ferraiuolo, L., McAlonis-Downes, M., Zou, Y., Drenner, K., Wang, Y., Ditsworth, D., Tokunaga, S., & Kopelevich, A. (2015). Translational profiling identifies a cascade of damage initiated in motor neurons and spreading to glia in mutant SOD1-mediated ALS. *Proceedings of the National Academy of Sciences of the United States of America*, 112(50), E6993–E7002.
- Sun, Y., Ouyang, Y.-B., Lijun, X., Chow, A. M.-Y., Anderson, R., Hecker, J. G., & Giffard, R. G. (2006). The carboxyl-terminal domain of inducible Hsp70 protects from ischemic injury in vivo and in vitro. *Journal of Cerebral Blood Flow and Metabolism*, 26(7), 937–950.
- Szalay, G., Martinecz, B., Lénárt, N., Környei, Z., Orsolits, B., Judák, L., Császár, E., Fekete, R., West, B. L., Katona, G., & Rózsa, B. (2016). Microglia protect against brain injury and their selective elimination dysregulates neuronal network activity after stroke. *Nature Communications*, 7, 11499.
- Tamura, A., Graham, D. I., McCulloch, J., & Teasdale, G. M. (1981). Focal cerebral ischaemia in the rat: 1. Description of technique and early neuropathological consequences following middle cerebral artery occlusion. *Journal of Cerebral Blood Flow and Metabolism*, 1(1), 53–60.
- Tang, Z., Gan, Y., Liu, Q., Yin, J.-X., Liu, Q., Shi, J., & Shi, F.-D. (2014). CX3CR1 deficiency suppresses activation and neurotoxicity of microglia/macrophage in experimental ischemic stroke. *Journal of Neuroinflammation*, 11, 26.
- Tassoni, A., Farkhondeh, V., Itoh, Y., Itoh, N., Sofroniew, M. V., & Voskuhl, R. R. (2019). The astrocyte transcriptome in EAE optic neuritis shows complement activation and reveals a sex difference in astrocytic C3 expression. *Scientific Reports*, 9(1), 10010.
- Thion, M. S., Ginhoux, F., & Garel, S. (2018). Microglia and early brain development: An intimate journey. *Science*, 362(6411), 185–189.
- Valny, M., Honsa, P., Kirdajova, D., Kamenik, Z., & Anderova, M. (2016). Tamoxifen in the mouse brain: Implications for fate-mapping studies using the tamoxifen-inducible Cre-loxP system. *Frontiers in Cellular Neuroscience*, 10, 243.
- van der Weerd, L., Lythgoe, M. F., Badin, R. A., Valentim, L. M., Akbar, M. T., de Belleruche, J. S., Latchman, D. S., & Gadian, D. G. (2005). Neuroprotective effects of HSP70 overexpression after cerebral ischaemia—An MRI study. *Experimental Neurology*, 195(1), 257–266.
- Vartanian, K. B., Stevens, S. L., Marsh, B. J., Williams-Karnesky, R., Lessov, N. S., & Stenzel-Poore, M. P. (2011). LPS preconditioning redirects TLR signaling following stroke: TRIF-IRF3 plays a seminal role in mediating tolerance to ischemic injury. *Journal of Neuroinflammation*, 8, 140.
- Villa, A., Gelosa, P., Castiglioni, L., Cimino, M., Rizzi, N., Pepe, G., Lolli, F., Marcello, E., Sironi, L., Vegeto, E., & Maggi, A. (2018). Sex-specific features of microglia from adult mice. *Cell Reports*, 23(12), 3501–3511.
- Virani, S. S., Alonso, A., Aparicio, H. J., Benjamin, E. J., Bittencourt, M. S., Callaway, C. W., Carson, A. P., Chamberlain, A. M., Cheng, S., Delling, F. N., Elkind, M. S. V., Evenson, K. R., Ferguson, J. F., Gupta, D. K., Khan, S. S., Kissela, B. M., Knutson, K. L., Lee, C. D., Lewis, T. T., ... Tsao, C. W. (2021). Heart disease and stroke statistics—2021 update: A report from the American Heart Association. *Circulation*, 143(8), e254–e743.
- Wang, Z.-Y., Leushkin, E., Liechti, A., Ovchinnikova, S., Mößinger, K., Brüning, T., Rummel, C., Grützner, F., Cardoso-Moreira, M., Janich, P., & Gatliff, D. (2020). Transcriptome and translome co-evolution in mammals. *Nature*, 588(7839), 642–647.
- Wu, F., Zhao, Y., Jiao, T., Shi, D., Zhu, X., Zhang, M., Shi, M., & Zhou, H. (2015). CXCR2 is essential for cerebral endothelial activation and leukocyte recruitment during neuroinflammation. *Journal of Neuroinflammation*, 12, 98.
- Yang, Y., & Rosenberg, G. A. (2015). Matrix metalloproteinases as therapeutic targets for stroke. *Brain Research*, 1623, 30–38.
- Yenari, M. A., Liu, J., Zheng, Z., Vexler, Z. S., Lee, J. E., & Giffard, R. G. (2008). Antiapoptotic and anti-inflammatory mechanisms of heat-shock protein protection. *Annals of the New York Academy of Sciences*, 1053(1), 74–83.
- Xie, L., Zhang, S., Huang, L., Peng, Z., Lu, H., He, Q., Chen, R., Hu, L., Wang, B., Sun, B., Yang, Q., & Xie, Q. (2023). Single-cell RNA sequencing of peripheral blood reveals that monocytes with high cathepsin S expression aggravate cerebral ischemia-reperfusion injury. *Brain, Behavior, and Immunity*, 107, 330–344.
- Yoon, H., Jang, Y. H., Kim, S. J., Lee, S. J., & Kim, S. K. (2015). Toll-like receptor 2 is dispensable for an immediate-early microglial reaction to two-photon laser-induced cortical injury in vivo. *The Korean Journal of Physiology and Pharmacology: Official Journal of the Korean Physiological Society and the Korean Society of Pharmacology*, 19(5), 461–465.
- Zamanian, J. L., Lijun, X., Foo, L. C., Nouri, N., Zhou, L., Giffard, R. G., & Barres, B. A. (2012). Genomic Analysis of Reactive Astroglia. *The Journal of Neuroscience: The Official Journal of the Society for Neuroscience*, 32(18), 6391–6410.
- Zhang, Y.-Y., Wang, K., Liu, Y.-E., Wang, W., Liu, A.-F., Zhou, J., Li, C., Zhang, Y. Q., Zhang, A. P., Lv, J., & Jiang, W. J. (2019). Identification of Key Transcription Factors Associated with Cerebral Ischemia-reperfusion Injury Based on Gene-set Enrichment Analysis. *International Journal of Molecular Medicine*, 43(6), 2429–2439.
- Zheng, K., Lin, L., Jiang, W., Chen, L., Zhang, X., Zhang, Q., Ren, Y., & Hao, J. (2022). Single-cell RNA-Seq reveals the transcriptional



landscape in ischemic stroke. *Journal of Cerebral Blood Flow and Metabolism*, 42(1), 56–73.

Zhu, A., Ibrahim, J. G., & Love, M. I. (2019). Heavy-tailed prior distributions for sequence count data: Removing the noise and preserving large differences. *Bioinformatics*, 35(12), 2084–2092.

#### SUPPORTING INFORMATION

Additional supporting information can be found online in the Supporting Information section at the end of this article.

**How to cite this article:** Hernandez, V. G., Lechtenberg, K. J., Peterson, T. C., Zhu, L., Lucas, T. A., Bradshaw, K. P., Owah, J. O., Dorsey, A. I., Gentles, A. J., & Buckwalter, M. S. (2023). Translatome analysis reveals microglia and astrocytes to be distinct regulators of inflammation in the hyperacute and acute phases after stroke. *Glia*, 71(8), 1960–1984. <https://doi.org/10.1002/glia.24377>